12-2011

EFFECT OF SELECTED PHASE CHANGE MATERIALS CONCENTRATION AND MANUFACTURING PROCESS ON THE PROPERTIES OF PLASTER MIXTURE SYSTEMS

Rong Cui
Clemson University, crong@clemson.edu

EFFECT OF SELECTED PHASE CHANGE MATERIALS CONCENTRATION AND MANUFACTURING PROCESS ON THE PROPERTIES OF PLASTER MIXTURE SYSTEMS

A Thesis
Presented to
the Graduate School of
Clemson University

In Partial Fulfillment
of the Requirements for the Degree
Master of Science
Polymer and Fiber Science

---

by
Rong Cui
December 2011

Accepted by:
Dr. Vincent Blouin, Committee Chair
Dr. Marian (Molly) Kennedy
Dr. Jian Luo

ABSTRACT

Phase change materials (PCM) are generally used in building construction materials for their ability to absorb and release large amounts of energy when their phase change happens at their specific melting temperature. This results in a significant increase in thermal mass of the building, a reduction in temperature fluctuations and therefore a reduction in heating and cooling loads. However, in order to properly select a PCM and optimize its integration in a specific building, the properties of building construction materials enhanced with PCM must be known. This research focuses on studying the effects of the concentration of a micro-encapsulated PCM on the physical, thermal, and mechanical properties of plaster mixtures. A series of gypsum wallboard samples with integrated Microtek 18D of varying concentration up to 40% in weight were prepared and analyzed using macro-scale analysis methods (i.e., thermal pile and flash method for measuring thermal conductivity, Thermogravimetric Analysis, Differential Scanning Calorimetry, and three-point bending test) and micro-scale analysis methods (i.e., Scanning Electron Microscopy, Energy Dispersive Spectroscopy) to evaluate the effect of PCM on the properties of gypsum wallboards, and the effect of the curing process on the properties of gypsum wallboards. The results suggest that the curing process has an impact on the effect of the PCM concentration on material properties.

DEDICATION

I appreciate both of my parents, my advisor, and all my friends who have been with me through this process for their endless encouragement and patience.

ACKNOWLEDGMENTS

First of all, I would like to give my sincerest gratitude to my advisor Dr. Blouin, for his constant support and advising. He motivated and assisted me in completing this degree. Without his continuous help, this work would not have been achieved. I would like to thank my committee members, Dr. Kennedy and Dr. Luo, for their guidance and advice. Secondly, I would also like to thank Dr. Shweisinger, for his assistance in the experimental set up. Last but not least, I owe my acknowledgments to Dr. Blouin's students for helping me with my research and building a friendly atmosphere: Claire Poh, Erick Koonz, Niraj Poudel, Nick Tritapoe, Esvar Subramanian, and Pengyu Chen.

TABLE OF CONTENTS

Table of Contents (Continued)

Page

LIST OF TABLES

LIST OF FIGURES

List of Tables (Continued)

Table Page

CHAPTER ONE

INTRODUCTION

1.1 Background

The building industry is known to be the largest energy consumption sector with more than 40% of the energy consumption and greenhouse gas emissions in the United-States [1]. The continuously increasing energy consumption drives wide research efforts on renewable resources and energy saving solutions in buildings [2, 3]. The major part of energy consumption in buildings is electrical energy due to heating, ventilation, and air-conditioning (HVAC), which varies by industrial, commercial or residential activity, extreme hot or cold climates, and time during the day [3]. Thus there is an increasing need of study on efficient energy storage HVAC systems. Among these approaches, natural energy source (i.e., solar energy) and thermal energy storage (TES) [4, 5] are considered two of the most promising ways to reduce thermal energy consumption. Solar thermal energy, concentrated solar power, biomass, cogeneration (i.e., combined heat and power), heat pumps and district heating are possible technologies that enable thermal energy storage. TES is a heat or cool storage that allows "thermal energy to be stored temporarily for later use" [1]. TES technologies can be categorized as sensible, latent and chemical. While sensible heat refers to thermal energy due to a change in temperature, latent heat is heat absorbed or release during a process (such as phase transition) without temperature change, and chemical heat is heat released or absorbed through chemical reactions. While the principle of sensible heat storage is to increase thermal capacity, the

principle of latent heat storage is based on phase change (such as melting and crystallization). Heat storage systems are characterized by their operating temperature, specific energy density, and the rate of energy storage.

Phase change materials (PCM) are considered a latent heat storage technology. By comparing with other types of technology including conventional thermal storage materials, PCMs have some distinct advantage [6,7]: applications in cold storage, overheat protection, comfort temperature control, and optimized building systems. However, only a few products are available on the market due to the lack of knowledge on how to efficiently integrate PCM to construction materials such as concrete, gypsum wallboard, and plaster.

PCM-enhanced building components have several anticipated advantages over conventional materials [7-9]: the ability to reduce energy consumption for space conditioning and reduce peak load, improvement of occupant comfort, compatibility with traditional technologies, and potential for applications in retrofit projects. A recent research project demonstrated that using PCM can achieve up to 25% energy savings in U.S. residential buildings [10]. Thus PCM-enhanced construction materials might have a high impact on the U.S. energy consumption.

Many factors influence the successful use of PCM. These includes which the type of PCM and amount of PCM, encapsulation method, and building system design are the most important. Thus a good understanding on the characteristics of PCM and its effect on construction materials are crucial to help architects and builders gain greater knowledge of potential energy savings and select appropriate design options.

Research on the application of PCM in buildings has a history of more than 50 years. In the 1940s, Telkes [10, 11] began to investigate the use of sodium sulfate decahydrate to store solar energy for space heating and solar energy storage in buildings. Since the 1970s and 1980s, several experimental approaches [7] were carried out on the application of different types of PCMs for solar energy storage, reduce peak loads and heating/cooling energy consumption. Since then, a considerable amount of relatively successful research efforts have been published that demonstrated the potential of PCMs for HVAC in various climate conditions [8]. Also, there has been some research on the development of new PCMs, the thermal properties of PCMs, the encapsulation of PCMs and numerical modeling. The function of PCM in buildings can be either passive, when PCM is included in building components, or active, when PCM is included in a circulating refrigerant for physically transporting heat to or from occupied building spaces. The goals of these two types of application of PCM in buildings are to make the best use of natural energy (mainly solar energy) for space heating and cooling [1]. This research focuses on passive applications, more specifically, on the integration of PCM in plaster gypsum boards.

Several commercial PCMs with specific properties have been developed for applications in buildings. These materials are generally encapsulated in polymeric micro-capsules, which allow them to be incorporated into construction materials. However, these products are few on the market due to the lack of knowledge on how to efficiently integrate PCM in construction materials [12]. In addition, there are no or limited national and international standards developed for integrating PCM into construction materials

[13]. Therefore, additional research is needed to understand how PCMs can impact the properties of these construction materials and increase their uses.

1.2 Research Objectives

This thesis is part of a larger project whose overall goal is to develop design guidelines for efficiently integrating PCM in buildings. This thesis focuses specifically on the characterization of the physical, thermal and mechanical properties of building construction materials enhanced with PCM, more specifically PCM-integrated gypsum wallboards. The goals of this research can be listed as follows:

- Conduct a review of the development of laboratory and commercial PCMs about their use as construction materials, and their characterization methods.
- Investigate the physical and thermal properties of different types of PCMs available (including Microtek 18D, Microtek 28D, Microtek 37D, Micronal DS5001) to evaluate their appropriate use in gypsum manufacturing. Products from these two manufacturers are selected due to their outstanding micro-encapsulation techniques which maintain the PCM thermally stable to a relatively high temperature.
- Use macro-scale analysis methods (i.e., thermal pile and flash method for measuring thermal conductivity, Thermogravimetric Analysis (TGA), Differential Scanning Calorimetry (DSC), and three-point bending test) and micro-scale analysis methods (i.e., Scanning Electron Microscopy (SEM), Energy Dispersive Spectroscopy (EDS)) to evaluate:

- the effect of PCM on the properties of gypsum wallboards, and
- the effect of the curing process on the properties of gypsum wallboards.

The effect of PCM is evaluated by varying its concentration in the gypsum-PCM mixture system. Different curing processes are studied in order to achieve an optimization of the properties and productivity.

1.3 Description of the Remaining Chapters

The second chapter provides a literature review on research in this field. The third chapter discusses the details of the experimental methods used to carry out this research on the PCM integration with gypsum, which covers the preparation and test methods of the materials. The fourth chapter provides experimental results and analysis. The fifth chapter includes the conclusions from the research and presents future work.

CHAPTER TWO

LITERATURE REVIEW

2.1 Introduction to Phase Change Materials (PCM)

Phase change material (PCM) is a type of latent heat storage (LHS) material. Unlike conventional materials, PCMs can be used to store and release a large amount of energy at a certain temperature at which their solid-liquid phase change occurs. When the ambient temperature of the PCM falls, the stored latent heat is released. To be considered for building applications, there are a wide variety of PCMs which have a melting temperature lying in the human comfort temperature range of 20° to 30°C. However, for their use in buildings, they need to meet thermal-dynamical and kinetic requirements, be chemically stable, nontoxic and non-corrosive. Moreover, cost also need to be taken into consideration.

The ideal PCM that can be used in thermal storage systems design should meet the following criteria [2]:

- Thermal dynamical properties
    - Proper phase-transition temperature
    - High latent heat
    - High specific heat
    - High thermal conductivity
- Kinetic properties
    - Minimum subcooling

        - Sufficient crystallization rate
- Physical properties
    - Appropriate density
    - Small volume change
    - Small vapor pressure
- Economic considerations
    - Large scale availability
    - Low cost

The melting point of PCM should be within the building operating temperature range. During daytime, when PCMs are heated to reach their melting temperature, they melt to liquid and absorb a large amount of heat from the environment while keep the temperature constant. When the temperature falls at night, the PCMs solidify and the stored latent heat is released to maintain the temperature constant. The latent heat and specific heat must be high to store a large amount of thermal energy and prevent subcooling. High thermal conductivity ensures the efficient charging and discharging of the stored energy. Subcooling of more than a few degrees may affect the efficiency of the system as it may shift the heat storage process out of the expected operating range [2]. A high enough density will allow a small size container. To reduce containment, small volume changes and small vapor pressure on phase transformation are required at operating temperatures. Thermal stability of PCM over time, which is related to the degradation of the PCM, is necessary to meet the life expectancy of the building. The

PCM should be nontoxic and noncorrosive to be safe for the human body and the environment. Also, availability and low cost of PCMs will dictate their use.

2.2 Classification of PCM

Generally, phase change materials are divided into three groups based on their composition: organic PCM compound, inorganic PCM compound, organic or inorganic eutectics [9]. A classification of PCMs is given in Figure 2.1.

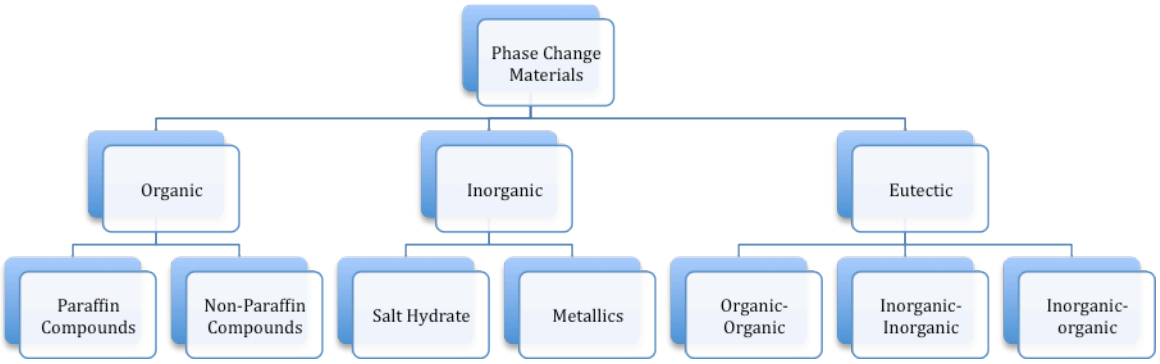

Figure 2.1 Classification of phase change materials [2]

The typical melting temperature range of each group is shown in Figure 2.2. From this figure it can be noticed that the melting point of several types of paraffin and salt hydrate lie in the comfortable room temperature, which make them appropriate for building applications. According to The American Society of Heating, Refrigerating, and Air-Conditioning Engineers (ASHRAE) [14], the comfortable room temperature has been listed for different types of buildings and environments. For instance, the comfortable

room temperature for a single office that has an occupancy ratio of 0.1 per square meter is listed as 21.1°C (70°F). An overview of phase change materials is given in Table 2.1 [15]. Many phase change materials are available in the required temperature range. However, a majority of phase change materials do not meet all the required criteria listed above.

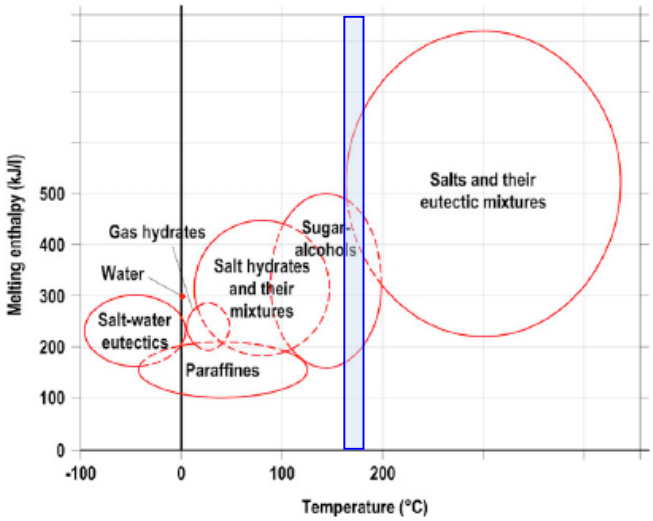

Figure 2.2 The melting enthalpy and melting temperature for the different groups of phase change materials (redrawn from [16])

Table 2.1 Overview of the main phase change materials [17]

Organic Compound	Paraffins	Inorganic compounds	(Inorganic) Eutectics
Polyglycol E 400	Paraffin C14	H_2O	58.7%$Mg(NO)_3.6H_2O$ + 41.3%MgCls
Polyglycol E 600	Paraffin C15-C16	$LiClO_3.3H_2O$	66.6%$CaCl_2.6H_2O$ + 33.3%$MgCl_2.6H_2O$
Polyglycol E 6000	Paraffin C16-C18	$Mn(NO_3)_2.6H_2O$	48%$CaCl_2$ + 4.3%NaCl +0.4%KCl +47.3H_2O
Dodecanol	Paraffin C13-C24	$LiNO_3.3H_2O$	47%$Ca(NO3)_2.4H_2O$ + 53%$Ma(NO3)_2.6H_2O$
Tetradodocanol	Paraffin C16-C28	$Zn(NO_3)_2.6H_2O$	60%$Na(CH_2COO).3H_2O$ + 40%$CO(NH_2)_2$
Biphenyl	Paraffin C18	$Na_2CO_3.10H_2O$	66.6%Urea + 33.4%NH_4Br
HDPE	Paraffin C20-C33	$CaBr_2.6H_2O$	
Trans-1,4-polybutadiene	Paraffin C22-C45	$Na_2HPO_4.12H_2O$	
Propianide	Paraffin C23-C50	$Na_2S_2O_3.5H_2O$	
Naphtalene	Paraffin wax	$Na(CH_3COO).3H_2O$	
Erthitol	Octadecane	$Na_2P_2O_7.10H_2O$	
Dimenthl-sulfoxide		$Ba(OH)_2.8H_2O$	
Capric acid		$Mg(NO_3)_2.6H_2O$	
Capricnic acid		$(NH_4)Al(SO_4).6H_2O$	
Laurinic acid		$MgCl_2.6H_2O$	
Miristic acid		$NaNO_3$	
Lakisol		KNO_3	
Palmitic acid		KOH	
Stearic acid		$MgCl_2$	
Acetamid		NaCl	
Propionamid		Na_2CO_3	
		KF	
		K_2CO_3	

Organic Compounds

Paraffin waxes generally have a structure of $CH_3(CH_2)_nCH_3$ which is mostly a straight chain. Paraffin waxes could release a large amount of heat during the

crystallization of the (CH_3)-chain. Both the melting point and the latent heat of alkane increases when the number of carbon atoms increases. Paraffins have several favorable characteristics [4] such as a wide range of melting temperatures from 20°C to 70°C and low vapor pressure in the melt. They do not undergo phase segregation and do not significantly degrade with thermal cycling. They are safe, reliable, predictable, less expensive and non-corrosive. However, they have some undesirable properties that limit their use such as their low thermal conductivity, non-compatibility with the plastic container and moderately flammable.

Non-paraffin organic compounds [4] include wide organic materials such as fatty acids (caprylic, capric, lauric, myristic, palmitic and stearic, which contain between 8 and 18 carbon atoms per molecule), esters, alcohols and glycols. Their melting temperature varies between 16°C and 65°C. However, they are relatively expensive [4].

Inorganic Compounds

Salt hydrates and metallics are two common types of inorganic compounds [2]. Salt hydrates are inorganic salts associated with water. They usually have good thermal storage density, high thermal conductivity and are available at a reasonable price. However, they may loose thermal storage capacity as they melt congruently. Supercooling and phase segregation might also limit their efficient use. Metallics are metal compounds that are not extensively considered as phase change materials due to their weight disadvantage. However, they still have some attracting features, such as high heat of fusion per unit volume and high thermal conductivity [17].

Eutectics

There are three groups of eutectics: organic-organic, inorganic-inorganic, and organic-inorganic. Eutectics are mixtures which consist of two or more components in proportions such that the melting temperature is lower than that of any mixture composed of the same constituents in other proportions. They have sharper melting peaks and slightly higher thermal storage density per volume than organic compounds. However, there is currently limited research focused on the thermo-physical properties of eutectics such as chemical composition, latent heat, and thermal stability.

2.3 PCM Integration into Support Materials

Cai *et al.* [18-20] prepared several PCM materials based on high density polyethylene (HDPE)/paraffin nano-composites with organophilic montmo-rillonite (OMT), expandable graphite (EG) and different additives using a twin screw extruder. Their chemical composition, latent heat, and thermal stability were investigated. Intercalation of paraffin into the layers was observed, and the incorporation of OMT, EG and other additives greatly influenced the fire resistance and thermal stability. Hong *et al.* [21] prepared a series of form-stable phase change material polyethylene (as supporting materials)-paraffin (as dispersed phase) compound (PPC). Different types of HDPE that has different melting index and density were blended with refined or semi-refined paraffin of different weight percentage. It was found that the type of HDPE, rather than mass percentage of the HDPE plays an important role in phase change behavior of the material. There is also no significant difference observed in the phase change range of the materials while using different types of paraffin.

Karaipekli *et al.* [22-24] continuously explored form-stable phase change materials for thermal energy storage. They first prepared expanded graphite (EG) and carbon fiber (CF)/stearic acid (SA) PCMs with different mass fractions and studied their thermal conductivity. The result indicated that thermal conductivity could be greatly improved by adding EG/CF while the latent heat storage capacity was not significantly reduced. Then they prepared a eutectic mixture of capric acid (CA) and myristic acid (MA) incorporated with expanded perlite (EP) and evaluated the chemical compatibility and thermal properties. The result indicated that the phase change temperatures of CA–MA/EP composite decreased, which can be due to "interaction between the carboxyl groups of CA and MA and the alkaline region in the EP such as K_2O, Na_2O, and CaO". Later, their group prepared another type of phase change material which was made of capric acid (CA) and myristic acid (MA) incorporated with vermiculite (VMT). Their research successfully increased the thermal conductivity of the paraffin and eutectics by the addition of EG, CF, and VMT. They also demonstrated improved thermal and chemical stability of these materials. Sari *et al.* [25-31], who are co-researchers of the previous group, carried out research on several microencapsulated PCMs for latent heat thermal energy storage, which include paraffin/EG, paraffin/HDPE, n-octacosane, PMMA/n-heptadecane, capric acid (CA)/palmitic acid (PA) eutectic mixture, CA/EP, and SMA/fatty acid composites (stearic acid (SA), palmitic acid (PA), myristic acid (MA) and lauric acid (LA) composites such as SMA/SA, SMA/PA, SMA/MA and SMA/LA). The thermal properties such as proper melting temperatures, high latent heat storage

capacities, and improved thermal conductivity indicate their promising applications in TES.

Wang [32] prepared and characterized fatty acid eutectic/polymethyl methacrylate PCM. The fatty acid eutectics were prepared by capric acid (CA), lauric acid (LA), myristic acid (MA) and stearic acid (SA) by self-polymerization. The fatty acid eutectics, CA–LA, CA–MA, CA–SA and LA–MA act as PCM while PMMA acts as the supporting material. There is no chemical reaction between the fatty acid eutectic and PMMA, and good compatibility between the fatty acid eutectic and PMMA was observed by FTIR. The latent heat and bending strength of these PCM demonstrated their potential use for energy saving in buildings.

Wang [33, 34] improved the thermal conductivity of polyethylene glycol (PEG)/Silica dioxide (SiO_2) composites by adding b-Aluminum nitride (b-AlN) powder, which has a higher thermal conductivity. They investigated the structure and thermal properties of the blends. The XRD pattern indicated a crystallite structure due to its close molecular packing and regular crystallization. Adding b-Aluminum nitride additive as a heat transfer promoter effectively improved the thermal conductivity of the material. However, latent heat decreased significantly.

Liu *et al.* [35] prepared a microencapsulated form-stable PCM consisting of paraffin (as PCM core) and inorganic silica gel polymer (as hydrophilic coating) in different weight percentage via in situ polymerization. It was observed that the hydrophilic–lipophilic properties of this material tested using Washburn equation could be improved with higher silica gel weight percentage, and phase change temperature

increased with a higher amount of paraffin, which is promising for fire resistant applications.

Zhang *et al.* [36, 37] tried to improve the thermal conductivity of form stable PCMs by introducing the same mass fraction of several kinds of additives among which exfoliated graphite was found to be most effective. The thermal conductivity increased with the mass fraction of exfoliated graphite, though the mechanical properties decreased. The experiment results matched well with numerical studies in the change of thermal conductivity. The same researchers then prepared n-tetradecane with different shell materials including acrylonitrile–styrene copolymer (AS), acrylonitrile–styrene–butadiene copolymer (ABS) and polycarbonate (PC) by phase separation method [38]. Low molecular weight microcapsules with high phase change enthalpies were obtained, but their mechanical properties remained poor.

2.4 Building Applications

PCM in Wallboard

Ahmad *et al.* [39] compared three different types of wallboards with PCM: "a polycarbonate panel filled with paraffin granulates, a polycarbonate panel filled with polyethylene glycol PEG 600, and a polyvinyl chloride (PVC) panel filled with polyethylene glycol PEG 600 and coupled to a vacuum isolated panel". Numerical simulation was conducted to compare with experiment results. Several experiments were set up to determine the heat response of wallboard products. The final results show that PVC panels filled with PEG 600 had a high heat capacity storage, which better fit the desired properties. Ahmad *et al.* [40] then studied the incorporation of PCM into light

envelopes, which are frequently used in buildings. They researched the different heat efficiencies of test-cell wallboard with and without PCMs by experiment methods and numerical simulation.

Manz *et al.* [41] investigated an external wall system composed of transparent insulation material (TIM) and translucent PCM ($CaCl_2 \cdot 6H_2O$), which "allows selective optical transmittance of solar radiation". Experiments and calculations confirmed that the use of PCM has a positive effect on the utilization of solar gains. It showed that the thermal-optical properties of this TIM PCM material were very promising.

Athenitis *et al.* [42] conducted an experimental and numerical simulation of PCM in building envelope materials. Gypsum wallboard impregnated with PCM was investigated under a full-scale outdoor test. The result showed that the temperature of the passive solar test room decreased significantly during daytime. It is effective in reducing energy consumption and peak load. Chen *et al.* [43] established a one-dimensional non-linear mathematical model to analyze the heat conduction of wallboard with PCM. It was found that the energy storage and releasing properties of PCM wallboard results in the improvement of indoor comfort, solar radiation utilization and at least 17% in energy savings during the heating season.

Heim *et al.* [44] studied the effect of the PCM on heat capacity of a PCM incorporated gypsum panels system. As PCM was used for the room lining, latent heat and the temperature of the air and surface were measured to compare with the gypsum plasterboard with no PCM. The energy required was also evaluated at the beginning and

at the end of the heating season. In conclusion, the PCM/gypsum panels resulted in considerable solar energy storage.

In Borreguero's research [45], experimental and mathematical model were built to test the Fourier heat conduction of different PCM concentration in the gypsum wall. The result showed that with the increase of PCM concentration and lower wall thickness, the thermal energy storage capacity increased. The thermal conductivity was independent from the PCM content. This research showed that the use of PCM in energy savings would be promising. Darkwa *et al.* [46] evaluated different phase change zones (narrow, intermediate, and wide) of laminated PCM drywall samples for passive-solar buildings. The result indicated that the PCM drywall sample with a narrow phase change zone performed most efficiently in utilizing heat energy and increased the minimum temperature at night. Yan [47] researched paraffin, including, n-heptadecane, n-octadecane, n-eicosane, 46# paraffin, 48# paraffin and liquid paraffin in different concentration, for the application of PCM in the building envelope. Their phase change temperatures and latent heat varied with their composition and proportion, which could be used as a reference for PCM to be used in buildings.

PCM in Concrete

Bentz *et al.* [48] studied pre-wetted light weight aggregates (LWA) filled with PCMs in concrete technology. The LWA has a relatively high porosity and heat absorption capacity, and they can be filled with PCM. Applications of PCM-filled LWA were investigated by experimental and numerical study: the increased energy storage capacity, reducing temperature rise which prevent cracking during the curing process,

and reducing the freeze/thaw cycles of concrete used in residential and commercial applications. Cabeza *et al.* [49, 50] developed concrete with PCM, which can achieve great energy savings in construction. They studied the thermal aspect of two real size concrete cubicles with PCM which has a melting temperature of 26.8°C. The result showed that adding PCM improved the thermal inertia as well as lowered the inner temperatures.

Hunger *et al.* [51] evaluated the behavior of self-compacting concrete containing micro-encapsulated phase change materials. After evaluating the properties of fresh concrete, different amounts of microencapsulated PCM were mixed into the concrete, which decreased the thermal conductivity and increased the heat capacity. Significant bending strength had been observed, and a large amount of PCM was destroyed during the manufacturing process. However, the mechanical properties still satisfied most applications.

PCM in insulation materials (foaming plastic) and other materials

Chen *et al.* [52-54] prepared several types of PCM composite fibers by electrospinning. They used polyethylene terephthalate (PET) as supporting materials, and a series of fatty acids, lauric acid (LA), myristic acid (MA), palmitic acid (PA), stearic acid (SA) and stearyl stearate (SS) as PCMs. It was showed that fiber diameter, the surface quality of fiber, and latent heat were greatly influenced by the PCM/polymer mass ratio, but the type of PCM contributed more to determine the phase change temperature and latent heat. These fibers were found to “have good stable and reliable thermal properties”. Chen *et al.* [55,56] also investigated ultrafine fibers of PEG/

cellulose composites. Polyethylene glycol/cellulose acetate (PEG/CA) composite were prepared by electrospining and its thermal storage and release properties were studied. A cylindrical structure with a smooth surface was obtained in which PEG distributes both on the surface and the core of the fibers. In their following research, the PEG/CA were prepared by crosslinking with toluene-2, 4-diisocyanate (TDI). The thermal stability was improved but enthalpy decreased.

Castell *et al.* [57] tested the properties of macroencapsulated phase change materials with conventional and alveolar brick in real conditions. The result showed that the PCM can reduce the peak temperature up to 18°C and apparently prevent heat fluctuation in summer, which resulted in a large amount of electrical energy savings and CO_2 emission reduction.

Other building applications of PCM focus on heat transfer enhancement [59, 60], pipe insulation [60-63], phase change material floors and roofs [65-68], and hybrid heating system [68, 69].

CHAPTER THREE

EXPERIMENTAL METHODS

This chapter provides the materials used and experimental procedures of this research. The materials that are used to study the effect of PCM on gypsum wallboard include plaster of Paris and four different types of PCMs. The PCMs were characterized to gain a better understanding of their chemical composition and properties by Fourier Transform Infrared Spectroscopy (FTIR) and optical microscopy. Thermogravimetric Analysis (TGA) and Differential Scanning Calorimetry (DSC) were applied to detect the thermal stability of the PCMs. Then MPCM 18D, which was demonstrated to be appropriate for the curing process, was used to conduct an experiment to reproduce the industrial manufacturing process of gypsum wallboards. The control parameters include the weight percentage of PCM, the addition of aluminum powder, and the temperature and duration of the baking stage of the manufacturing processes. Other additives such as starch, glass fiber, and foaming agents are not added in this research in order to maximize the effect of PCM. However, these additives are suggested to be studied in the future.

3.1 Preparation of Gypsum Wallboard with PCM

3.1.1 Materials

(a) Plaster of Paris

The plaster of Paris (product name: USG® White Moulding Plaster) [70] was obtained from United States Gypsum Company. The material contains 95% plaster of Paris ($CaSO_4 \cdot nH_2O$, n=0.5-0.8) and 5% Crystalline Silica.

(b) PCM

The four types of PCMs used were purchased from Microtek Laboratories and from BASF [71, 72]. As illustrated in Figure 3.1, these PCMs have a micro-encapsulated structure which consist of 85-90% PCM core, which usually are alcanes, and 10-15% polymer shell (which is listed as proprietary). Microencapsulation is a process to embed droplets of PCM into a spherical coating or shell. The micro-encapsulation technology has several advantages, such as preventing leakage and maintaining the PCM thermally and structurally stable. Research on PCMs encapsulated into shells of other shapes such as irregular shape, multi-walled PCM, and cores embedded in a matrix, or multi-cores PCM do exist [73]. However, the spherical PCMs are the most common among the different shapes due to its more convenient preparation and applications. The polymer shell is used to contain the PCMs when melted. The Microtek products are MPCM 18-D, MPCM 28-D, MPCM 37-D, which are named based on their melting temperature of 18°C, 28°C, and 37°C, respectively. The BASF product is Micronal® DS 5001 which has a melting temperature of 26°C. These PCMs exist as white dry powder similar to flour. The physicals properties of the PCMs are listed in Table 3.1.

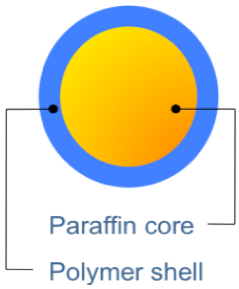

Figure 3.1 Microencapsulated PCM structure

The chemical composition and physical properties listed on their product technical data sheet are given in Table 3.1.

Table 3.1 Listed chemical composition and physical properties of PCM used in this research [72, 73]

Product Number	Melting Point (C)	Latent Heat (kJ/kg)	Density (g/cm3)	Core Material	Particle Size (micron)	Thermal Stable Temperature
MPCM 18D	18	163 to 173	0.9	n-Hexadecane	17 to 20	250
MPCM 28D	28	180 to 195	0.9	n-Octadecane	17 to 20	250
MPCM 37D	37	190 to 200	0.9	n-Eicosane	17 to 20	250
Micronal DS5001	26	110	0.25-0.35	n-Alcane	Not applicable	Not applicable

Fourier Transform Infrared spectroscopy (FTIR) analysis was done on the four PCMs using a Thermo-Nicolet Magna 550 FTIR in order to determine the chemical compositions of both the core and the polymer shell materials. The scans were done by a previous Master's student (i.e., Esvar Subramanian). However the analysis of the scan data was done in this research and is presented in this thesis. FTIR [74] is used to identify functional groups of unknown substance by measuring the infrared spectrum of a substance. A list of possible bonds can be identified by comparing the experimental absorption spectrum with literature database. Multiplex techniques, i.e., gas chromatography-infrared spectrometry-mass spectroscopy (GC-IR-MS), and thermogravimetry-infrared spectrometry (TG-IR) open up possibilities to get more accurate information of substances.

Figure 3.2 shows the FTIR graphs of the chemical composition of the Microtek 18D MPCM and BASF Micronal DS5001.

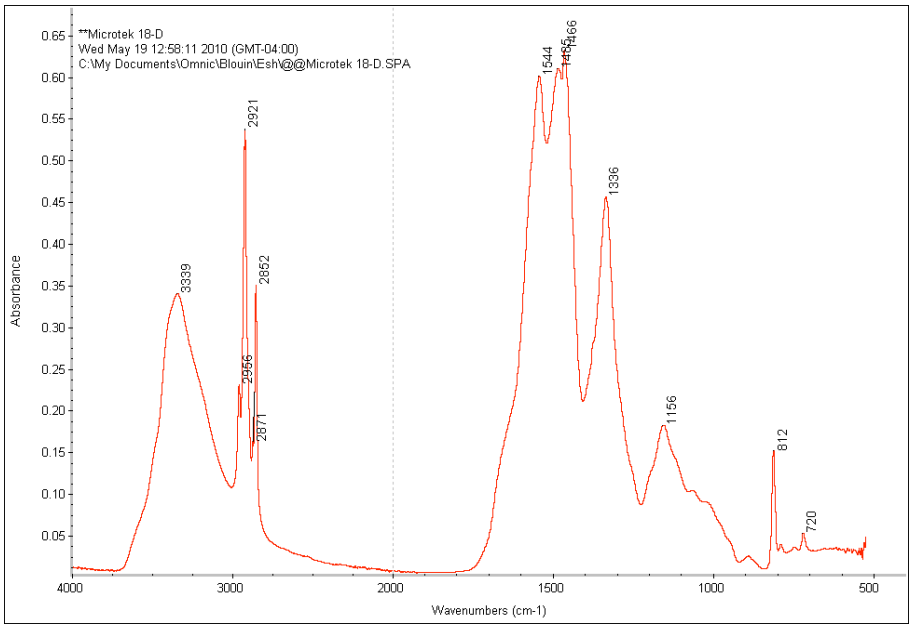

(a) Microtek PCM 18D

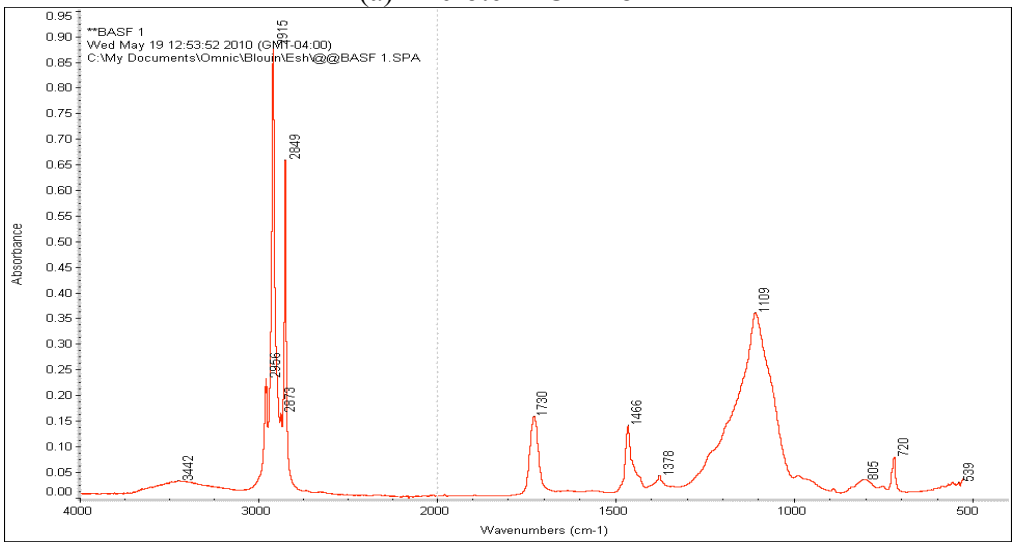

(b) BASF Micronal DS5001

Figure 3.2 FTIR spectrum of PCMs

The FTIR results of the functional group that the PCMs included were identified and listed in Table 3.2

Table 3.2 FTIR analysis of the PCMs [74-77]

Sample name	Significant Peaks at wavenumber (cm^{-1})	Related Functional Groups
Microtek 18D	3339	O-H stretch
	2956	N-H stretch
	2921	C-H stretch
	2852	C-H stretch
	1544	C=O stretch, N-H stretch
	1495	N-H stretch
	1493	N-C-N stretch
	1485	O-H stretch
	1466	$-CH_2-$ (deformation) stretch
	1336	$-CH_2-$ wagging
	1017	$-CH_2-OH$
	1156	-N-C-N stretch, C-O-C of $-CH_2-O-CH_2-$
	812	C-N bending
	720	C-H bending
Micronal DS5001	3442	O-H stretch
	2915	C-H stretch
	2849	C-H stretch
	1730	C=O stretch
	1466	C-H stretch
	1378	C-H stretch
	1109	C-O stretch
	720	-CH- bending

For the Microtek 18D PCM, the spectrum of Hexadecane was subtracted from the graph to extract the chemical composition of the polymer shell. According to the library search, the remaining spectrum matches the chemical Melamine-urea-formaldehyde to a degree of 81.37%, which is sufficient to conclude a match. Also, the chemical composition of BASF Micronal matches the structure of Monoglyceride and Diglyceride

to 82.23%. These FTIR peaks match the result of several published papers that successfully prepared and characterized PCM with melamine-formaldehyde shell [75-77].

The particle sizes of the PCMs were measured using the optical microscope Olympus BX60 as showed in Figure 3.3. The particle size and its distribution were measured to acquire information about how the particles would mix with the particles of plaster.

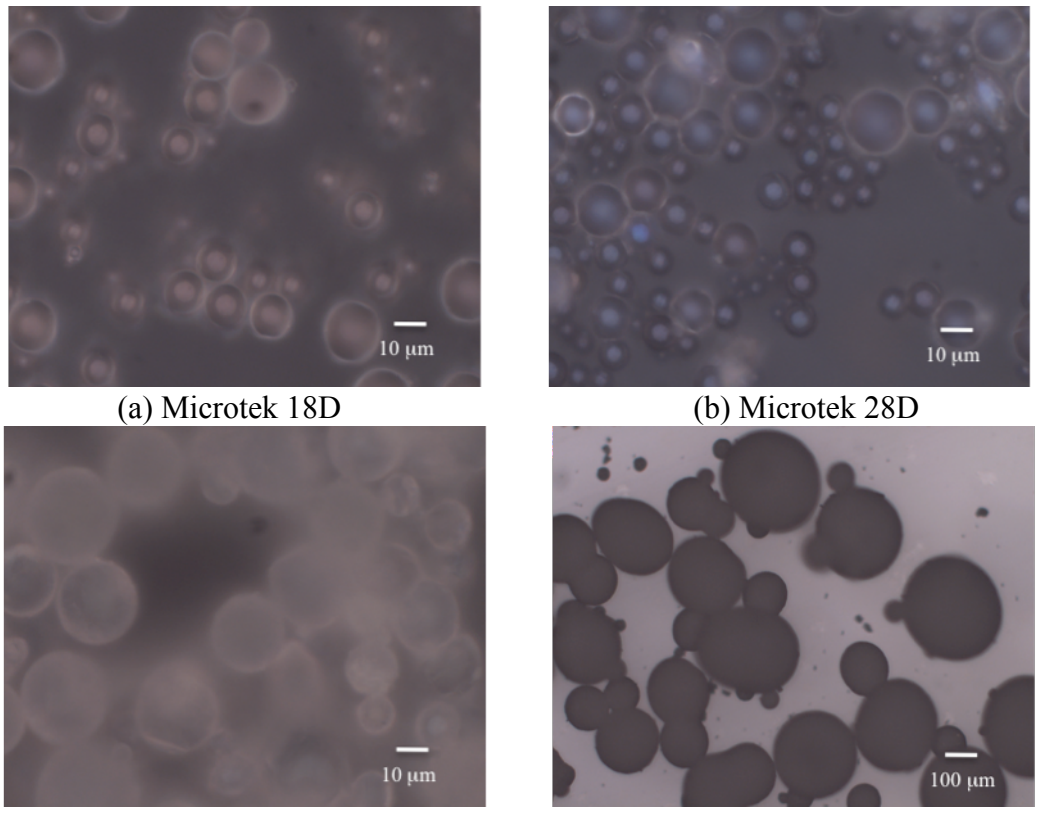

(a) Microtek 18D (b) Microtek 28D

(c) Microtek 37D (d) BASF Micronal DS5001

Figure 3.3 Optical microscope image of PCM (5X). The particles of the BASF product (d) are about 10 times larger than those of the Microtek products.

The measured diameter (mean) of these four PCMs listed in Figure 3.3 are: 6.26 μm, 9.20 μm, 23.03 μm, 182.00 μm, respectively. The particles have a large size range by comparing their standard deviations, which are 6.05μm, 3.37μm, 4.42μm, and

101.54μm, respectively, with their average diameter. These values match the information listed on their technical data sheet. Figure 3.4 shows the particle distribution of the PCMs. Sizing of particles was done by manually counting of particles of specific size ranges under optical microscope. It is observed that the BASF particles are about 20 times larger then the Microtek PCMs, so it is suspected that they would have a different effect on the mixture compared with the Microtek PCMs, which has similar size to the plaster particles.

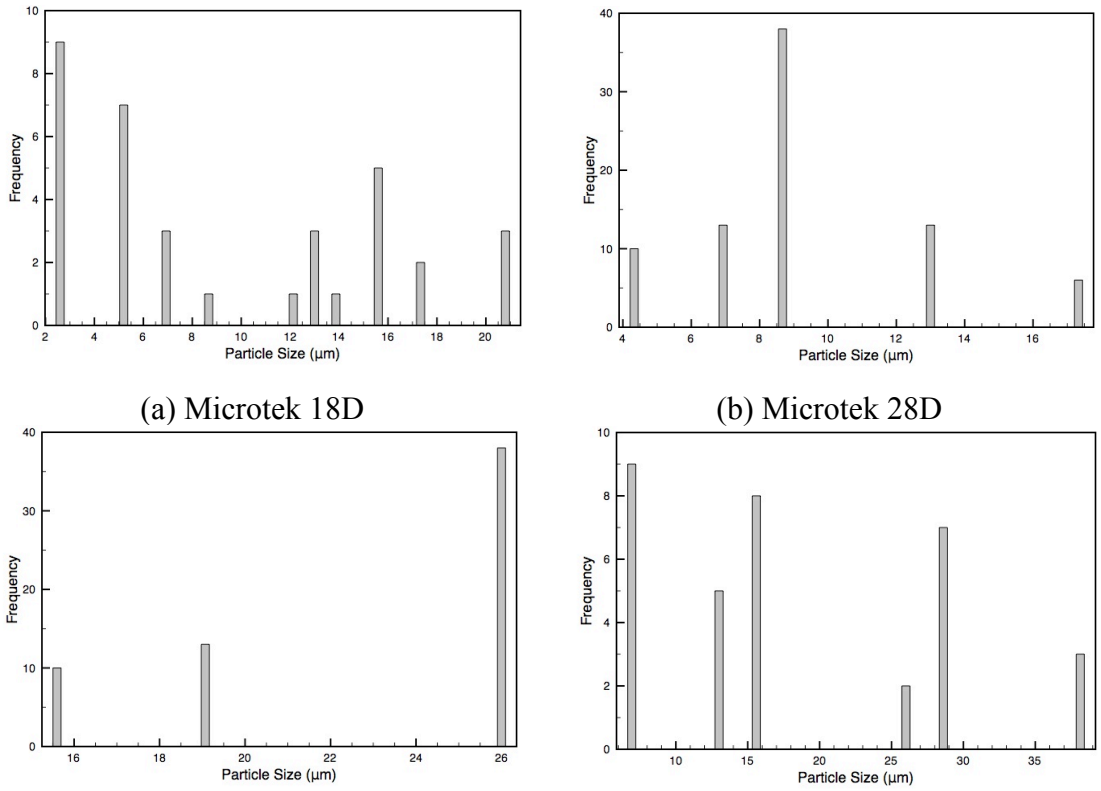

(a) Microtek 18D (b) Microtek 28D

(c) Microtek 37D (d) Micronal DS5001

Figure 3.4 Particle distribution of PCM

Thermogravimetric analysis (TGA) was run using a TA Instruments 2950 TGA to determine the degradation temperature of the PCM in order to ensure that it can survive

the baking stage, which requires a temperature of 260^{o}C, of the manufacturing process of gypsum plaster boards. TGA [78] is carried out to record weight change in relation to temperature change. The equipment consists of a microbalance, a pan (usually Platinum) loaded with the sample placed in a small oven with thermocouple to measure the temperature accurately. The samples were heated to 800°C at a heating rate of 10°C/min in an inert atmosphere (N_2). The weight percentage-temperature curve was created as shown in Figure 3.5.

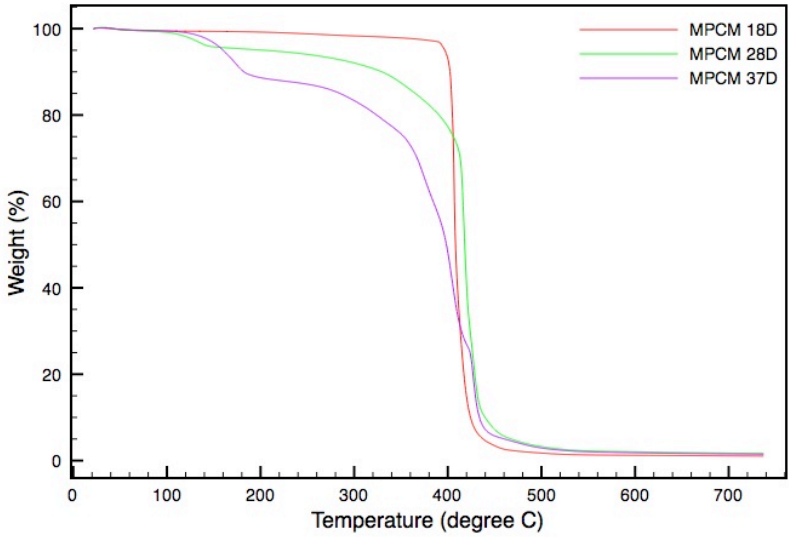

(a) Microtek MPCM

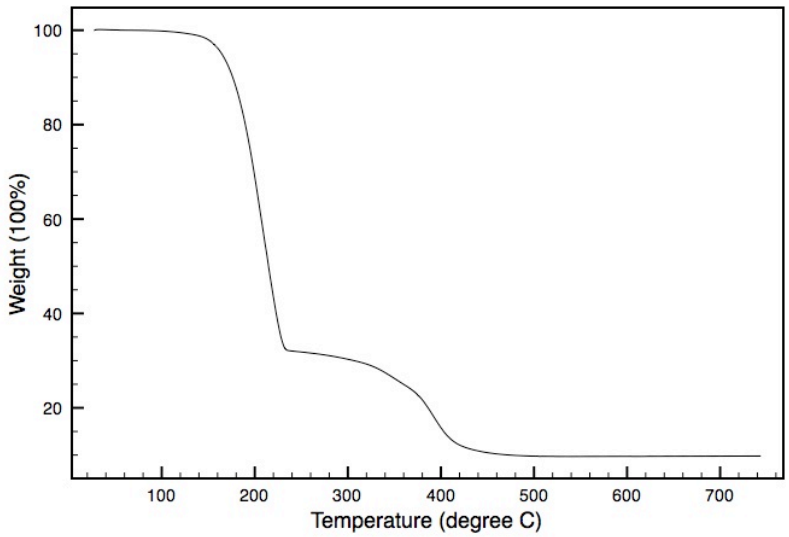

(b) Micronal DS5001

Figure 3.5 TGA results

The results show that only Microtek MPCM 18D degraded less than 5% when heated at 260°C, which means that it is the only PCM among the four tested that could handle the manufacturing process without degradation.

Also, isothermal TGA was conducted to evaluate the decomposition reaction at a constant temperature. The isothermal TGA was run on the same equipment and condition to detect whether the sample lost weight when the temperature was maintained at a particular temperature (260°C). After being heated to this temperature at a rate of 10°C/min in an inert atmosphere (N_2), the weight percentage-temperature curve was created as shown in Figure 3.6.

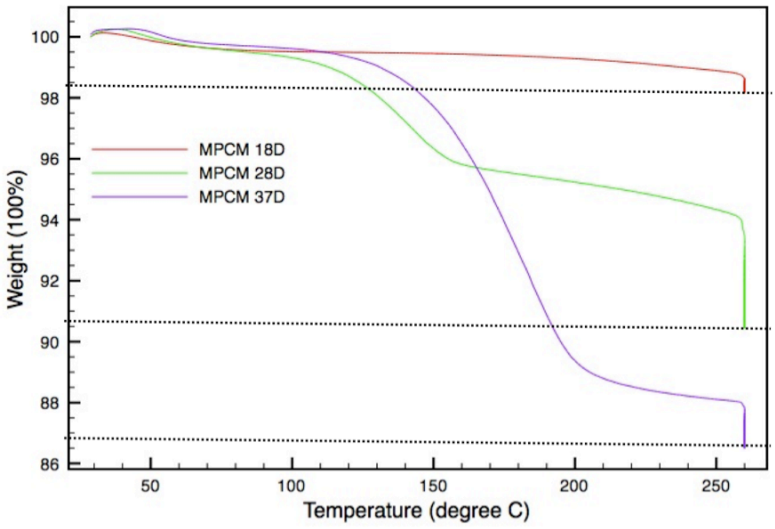

(a) Microtek MPCM

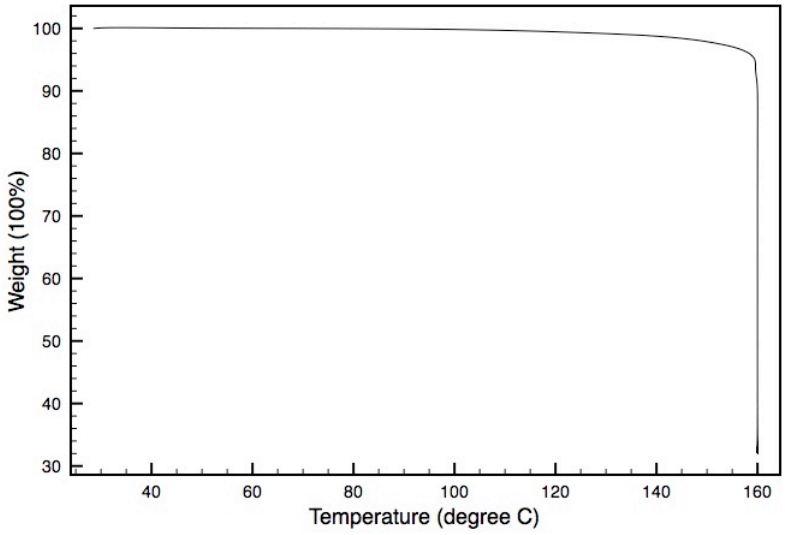

(b) Micronal DS5001

Figure 3.6 Isothermal TGA at 260°C of PCM

The isothermal TGA results agree with the TGA results and confirm that only Microtek MPCM 18D can be used up to 260°C. The weight loss from 100°C to 200°C is mainly due to the core proliferation while the weight loss at a higher temperature is due

to the "formation of the higher thermal stability of cross-linked polymer yielded by the core material" as described the research of Tong [76].

The detailed thermal behavior of MPCM 18D was detected by TA Instruments Q1000 DSC. Samples (less than 10mg) were heated at a constant rate of 10°C/min to 260°C in a N_2 atmosphere to detect the phase transition of both the alcane core and polymer shell of the PCM.

DSC analysis was used to determine the energy storage ability of PCM. The principle of DSC [79] is to measure the difference in the amount of heat flux of a sample and a reference required to maintain the same temperature of the sample and the reference (which is mostly made of certified Indium metal), when they are heated or cooled at a constant rate. The difference of heat absorbed or emitted between the reference and the sample is then recorded as a curve versus temperature or versus time. DSC is used to observe melting temperature and latent heat of PCM during the exothermic or endothermic phase transition process. DSC has been applied to conduct accelerated thermal cycling test by measuring the melting point and latent heat of fusion "in the laboratory with a hot plate or similar system" [80]. According to the second law of thermodynamics, specific heat capacity can be determined by the amount of transferred heat:

$$\delta H = c_p \cdot m \cdot \delta T \tag{1}$$

The results are shown in Figure 3.7.

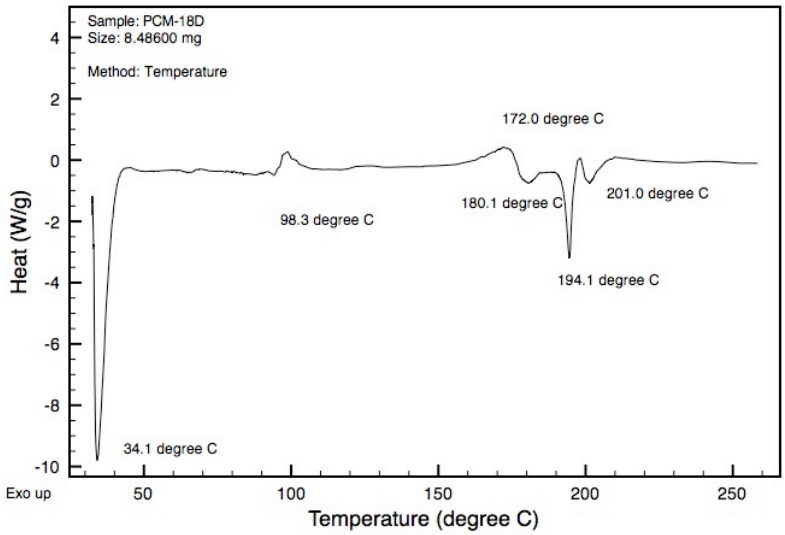

Figure 3.7 DSC curve of MPCM 18D

Melting peaks of the Alcane core of the PCM can be observed at 34.1 °C. The three distinct exothermic peaks at 180.1°C, 194.1°C, and 201.0°C may result from the "repaid polymerization reaction of core material triggered by the urea-derivatives and the gaseous products" released by the polymer shell, and the thermal decomposition of the polymer shell followed by its self-etherification. This result is very similar to that of Tong's research [81]. Since this PCM has a listed melting temperature of 18^{o}C, the melting peak of 34.1^{o}C, which is too high for this material, is suspected to be due to experimental inaccuracies and limitations at low temperature. The encapsulation of PCM prevents it from catching on fire easily.

(c) Additives

The aluminum used to control thermal behavior of plaster board samples is 99.5% pure aluminum and consists of particles 30 micrometers in diameter and smaller.

3.1.2 Procedure for Making PCM-Integrated Drywall Samples

The industrial production of gypsum wallboards can be achieved in four steps: mixing, forming, drying, and finishing [82, 83]. The first step is mixing the gypsum powder with additives, such as starch, paper pulp, unexpanded vermiculite, glass fiber, water, emulsion, and foaming agent. The mixture is poured onto a large board machine. In this machine, there are two layers of unrolling paper on the upper side and the bottom side, which make the slurry a "sandwich" structure. The sandwich then passes through a roller system to make the product to appropriate thickness. After setting, the panel is put into an oven at 500°F (260°C) in which temperature and humidity are carefully controlled. The panels are heated at this temperature for 35-40 minutes in order to remove excess water. After this process, more than 95.5% of water is evaporated. Also, the water evaporated will leave the panel through pores that account for more than 50% of the volume on average. Finally, the edges are finished using the automated assembly lines and cutting the panels. This process is showed in Figure 3.8.

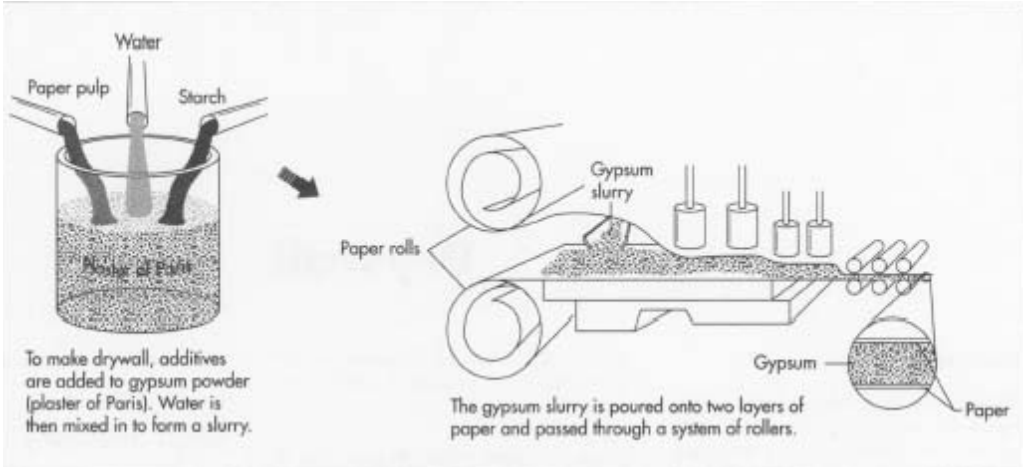

Figure 3.8 Industrial manufacturing process of gypsum wallboard [82, 83]

The main chemical reaction that occurs during this process corresponds to the powder hemihydrate ($CaSO_4.1/2H_2O$) that reacts with water and forms less soluble (interlocking crystalline) dihydrate ($CaSO_4.2H_2O$) as follows,

$$CaSO_4.1/2H_2O + 1\text{-}1/2H_2O \rightarrow CaSO_4.2H_2O \quad (2)$$

This is an exothermic reaction in which there is an induction period happening in the setting reaction during which the mixture is stirred and fills the mould. This is followed by the curing process, which dries the plaster as a solid and makes the sample ready to be removed from the mould.

However, it is difficult to reproduce the industrial manufacturing process in laboratory due to lack of proper equipment, such as a board and rolling machine. An attempt was to make samples manually by controlling the quantities of the ingredients and the time and temperature of the curing process. This procedure can be achieved as follows: the plaster powder, PCM and the other additives were weighted separately with precision of 0.1g and then uniformly mixed with the addition of 50% water in weight of the mixture. After stirring the material for 3 to 5 minutes, the resulting mixture was poured into 120mm x 55mm x 45mm corrosion-resistant moulds. After 10 minutes, the mixture was placed into a resistance oven Furnace-Linberg BF51733C for the curing process (i.e., baking stage).

The controlled parameters in this research include:

(a) The concentration of PCM. PCM varied from 0, 10, 20, 30 and 40% in weight of the mixture system before water was added to study the effect of PCM concentration on the mechanical and thermal properties of plaster wallboard integrated with PCM.

(b) Additive of Aluminum powder. 2% of Aluminum powder in weight was attempted to control the thermal behavior of the samples due to its apparently higher thermal conductivity (250 W/(m.K) compared to 0.17 W/(m.K) of gypsum powder).

(c) Manufacturing Process. Four different curing processes were studied in this research: (1) Curing the sample at 260°C at the rate of 10°C/min for 40 minutes; (2) Curing the sample at 240°C at the rate of 10°C/min for 50 minutes; (3) Curing the sample at 100°C at the rate of 10°C/min for 3 hours; (4) Curing the sample at 60°C at the rate of 10°C/min for 24 hours. It should be noted that the temperature and curing time had to be adjusted to have the similar effect as the conventional manufacturing process. The duration of baking was increase with decreasing temperature. Since the temperature of processes (1) and (2) was above the flash point of the alcane (i.e., 130^{o}C), aluminum was only added to the systems (3) and (4) in order to reduce the risk of the samples catching on fire. All the samples were then cut and polished to dimensions of 1mm x 50mm x 10mm for characterization.

Tables 3.3 and 3.4 list the final mixture compositions for each process. The quantities listed in these tables are the mass of materials mixed before curing. The PCM percentage labels (i.e, 0%, 10%, 20%, 30% and 40%) are approximate percentages that correspond to the weight percentage of PCM of the plaster/PCM mixture without water. For instance, the 20% PCM sample #3 for Process 1 includes 120g of plaster and 30g of PCM. The total mass of the plaster/PCM mixture without water is 150g, which leads to a 20% concentration of PCM.

Table 3.3 Mixture compositions without Aluminum powder

Process 1 260°C/40min

Sample #	**1**	**2**	**3**	**4**	**5**
PCM%	**0**	**10**	**20**	**30**	**40**
Plaster (g)	150	135	120	105	90
Water (g)	75.0	75.2	74.8	75	74.9
PCM (g)	0	15	30	45	60

Process 2 240°C/50min

Sample #	**1**	**2**	**3**	**4**	**5**
PCM%	**0**	**10**	**20**	**30**	**40**
Plaster (g)	120	108	96	84	72
Water (g)	60	60	75.4	76	80.1
PCM (g)	0	12	24	36	48

Process 3 100°C/3h

Sample #	**1**	**2**	**3**	**4**	**5**
PCM%	**0**	**10**	**20**	**30**	**40**
Plaster (g)	120	108	96	84	72
Water (g)	60	60	75.6	75.6	79.1
PCM (g)	0	12	24	36	48

Process 4 60°C/24h

Sample #	**1**	**2**	**3**	**4**	**5**
PCM%	**0**	**10**	**20**	**30**	**40**
Plaster (g)	120	108	96	84	72
Water (g)	60	60	76	75.5	80
PCM (g)	0	12	24	36	48

Table 3.4 Mixture compositions with Aluminum powder

Process 3 100°C/3h

Sample #	**1**	**2**	**3**
PCM%	**0**	**40**	**40**
Al%	**0**	**0**	**2**
Plaster (g)	120	72	69.6
Water (g)	60	100	100
PCM (g)	0	48	69.6
Al (g)	0	0	2.4

Process 4	**60°C/24h**		
Sample #	**1**	**2**	**3**
PCM%	**0**	**40**	**40**
Al%	**0**	**0**	**2**
Plaster (g)	120	72	69.6
Water (g)	60	100	100
PCM (g)	0	48	69.6
Al (g)	0	0	2.4

3.2 Experimental Characterization of Properties

Various macro-scale and micro-scale tests were conducted to investigate the properties of PCM integrated plaster wallboard samples.

3.2.1 Macro-scale Characterization

Physical Property: Density, Water Content and Porosity

The density of the prepared samples was calculated by dividing the mass by the volume of each sample.

The water content and porosity are then calculated based on the values of density. Water content represents the mass of water remaining after being cured. Water content u (%) can be calculated by the following equation:

$$u=m_w/m_b \quad (3)$$

where m_w is the mass difference between the initial amount of water added and water evaporated during heating, and m_b is the total mass of the sample.

The porosity of the sample is determined as the fraction of void space over the total volume of the sample [84].

$$\phi = V_V / V_T \quad (4)$$

where ϕ (%) is the porosity, which is the fraction of the volume of void-space V_V and the total or bulk volume of material V_T . The pore volume can be measured by the "water evaporation method" [83], in which pore volume is the weight difference between the saturated sample and the dried sample divided by the density of water. Then this value is modified by taking into account the measured volume change between before and after drying.

Mechanical Properties: Stiffness and Strength

Flexural properties of gypsum panel products were evaluated using a three-point bending system. This test was used to determine the flexural (bending) strength and the stiffness. The three point bending beam is showed in Figure 3.9 as following.

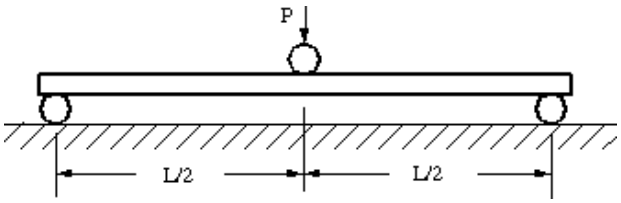

Figure 3.9 Three point bending beam

In this test, the geometry of materials and strain rate are important experimental parameters. The flexural stress, σ_f, strain ε_f and modulus E_f can be calculated using the following equations [85]:

$$\sigma_f = \frac{3PL}{2bd^2} \quad (5)$$

$$\varepsilon_f = \frac{6Dd}{L^2} \quad (6)$$

$$E_f = \frac{L^3 m}{4bd^2} \quad (7)$$

- σ_f = Stress in the outer surface at the midpoint, (MPa)
- ε_f = Strain in the outer surface, (mm/mm)
- E_f = Flexural modulus, (MPa)
- P = Load at a given point on the load deflection curve, (N)
- L = Length of the support span, (mm)
- b = Width of the test beam, (mm)
- d = Depth of the test beam, (mm)
- D = maximum deflection of the center of the beam, (mm)
- m = The gradient (i.e., slope) of the initial straight-line portion of the load deflection curve, (N/mm)

The stiffness and strength of the PCM integrated plaster wallboard samples were measured using a three-point bending machine, shown in Figure 3.10. It was installed with the help of Dr. Shweisinger based on modified ASTM C473 (Standard Test Methods for Physical Testing of Gypsum Panel Products) [86]. This machine could bear up to 50 lb force.

Figure 3.10 Three-point bending testing machine

In this test, the precision of the measurement is limited by the accuracy of the equipment. There are two main sources of error: the force measurement error and the displacement measurement error. An effective way to ensure the equipment is set up correctly is to record the zero point of the force measurement and to use a video camera to monitor this fracture experiment. The other unavoidable error may come from the place of the tip, which is marked and is reset before each measurement is taken. Also, the three point bending test is very sensitive to the testing specimens and their geometry. The experimental results were modified to account for the dimension of each specimen. The presence of air bubbles in the samples and inhomogeneity may also cause discrepancy in the results.

Thermal Properties: Thermal Conductivity and Thermal Diffusivity

Thermal conductivity is an important property, which characterizes the rate of conduction of thermal energy through the material. It can be measured using a steady-state method (absolute method) or transient techniques [87]. In a steady-state method, "a temperature gradient across the sample is measured in response to an applied amount of heating power", which usually measures the heat flow through the sample [88]. According to the Fourier's Law of thermal conduction, the heat flux density, which is "the amount of heat energy passed through a unit area per unit time", is equal to the product of thermal conductivity and the negative local temperature gradient, as:

$$q = -k\nabla T = -k\Delta T / L \tag{8}$$

where

- q= the local heat flux density ($W \cdot m^{-2}$),
- k= the material's conductivity, ($W \cdot m^{-1} \cdot K^{-1}$),
- ∇T= the temperature gradient ($K \cdot m^{-1}$),
- ΔT= the temperature difference (K),
- L= the thickness of the specimen (m).

For a plate of thermal conductivity k, area A and thickness L, thermal conductance is kA/L, measured in $W \cdot K^{-1}$.

Thermal conductivity was measured based on the ASTM standard C518-04 [88] (Standard Test Method for Steady-State Thermal Transmission Properties by Means of the Heat Flow Meter Apparatus). This method measures steady state thermal transmission through flat specimens by using a heat flow meter apparatus. This test method could be used to efficiently determine the thermal conductivity of a wide range of

materials with high accuracy once appropriate calibration in thermal conductance, dimensions, mean temperature and temperature gradient was carried out.

The general equipment set up is shown as Figure 3.11 as follows.

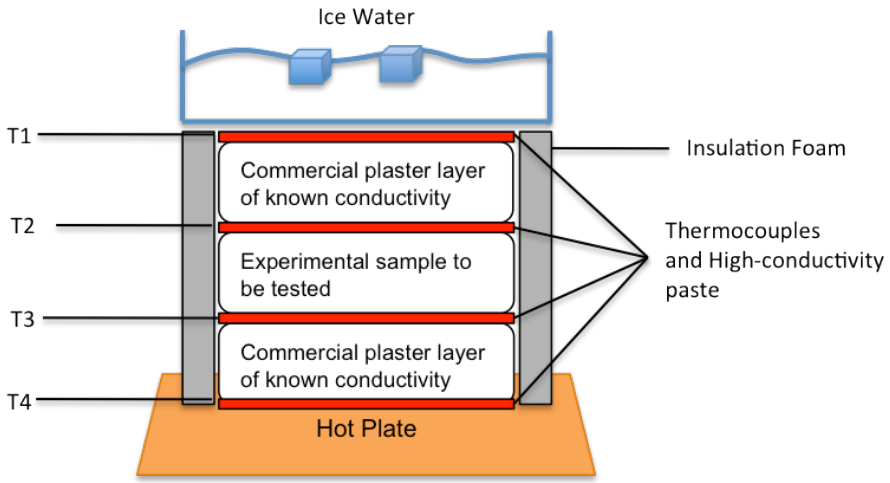

Figure 3.11 Thermal pile experimental set-up for measuring thermal conductivity

The apparatus is referred to as a thermal pile as it consists of a series of layers, namely, a hot plate (i.e., heat source), a 1000 ml beaker filled with ice water as cold plate (i.e., heat sink), and the sample to be tested sandwiched between two commercial plaster layers of known conductivity. The hot plate was set to 60°C which is above the melting temperature of the PCM and the cold plate was maintained at 0°C. Four type-K thermocouples were used to measure the temperature at the four interfaces between the hot plate, the commercial layers and the sample. The thermocouples were connected to an Analog/Digital Input/Output InstruNET® data acquisition system to record the temperatures as functions of time, as shown in Figure 3.12. A set of double-layered Styrofoam insulation walls was used around the three central layers in order to prevent heat loss.

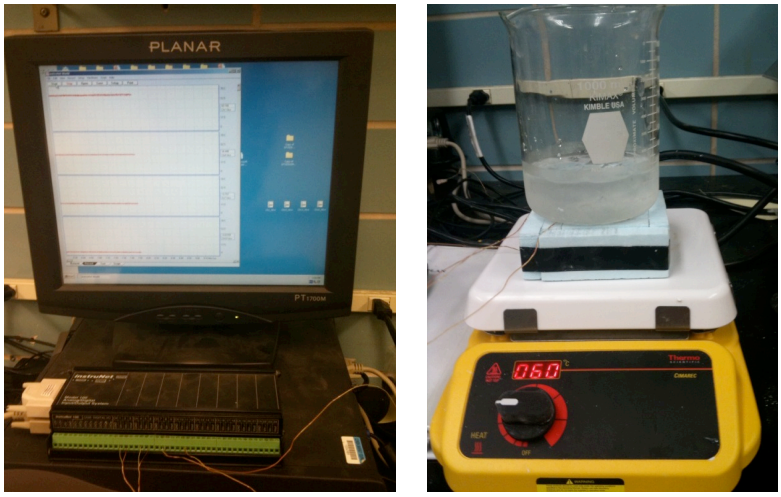

Figure 3.12 Thermal conductivity equipment

The three layers of specimens consist of two commercial products and one experimental sample. The experimental specimens for the thermal conductivity test were acquired from the broken pieces of the three point bending test. All samples were cut and polished to dimensions of 50mm x 50mm x 10mm.

Neglecting heat losses, the heat fluxes through the three layers should be mutually equal, as defined in the standard, as long as all samples and layers of known conductivity are produced with the same dimensions. The thermal conductivity of the sample can be calculated by direct comparison with samples of known conductivity. If the temperatures at the four interfaces are noted T_1, T_2, T_3, T_4, the condition of equal heat fluxes through the three layers can be written as:

$$k_o(T_2-T_1)/L_o = k(T_3-T_2)/L = k_o(T_4-T_3)/L_o \quad (9)$$

where

k_o = known conductivity of the two commercial layers, namely $k_o = 0.17$ W/(m.K);

k = unknown conductivity of the sample;

L_o = thickness of the two commercial layers;

L = thickness of the sample;

T_1 to T_4 = temperatures at the four interfaces.

From this equation, the conductivity of the sample can be estimates as:

$$k = k_o(T_2-T_1)L/((T_3-T_2)L_o) = k_o(T_4-T_3)L/((T_3-T_2)L_o) \quad (10)$$

The thermocouples are first calibrated by attaching them to the hot and cold plate to ensure they provide temperature readings (less than 5% difference). After steady state is reached (after around 10 minutes), the average temperatures were recorded. The main source of error of this test is due to the non-uniform dimensions of the samples and their surface roughness. High temperature high thermal conductivity paste (Omegatherm 201) was used between each layer in order to reduce the effect of gap conductance. Additional experimental error is due to the potential presence of bubbles in the samples. Finally, the insulation does not prevent all heat loss perfectly during the measurements.

The experimental results can be compared with the thermal conductivity predicted by Maxwell's relation [89, 90].

$$\kappa_{eff} = \kappa_p \frac{\kappa_m(1+2\delta_m) - \kappa_p(2\delta_m - 2)}{\kappa_p(2+\delta_m) + \kappa_m(1-\delta_m)} \quad (11)$$

where κ_{eff} is the effective thermal conductivity of the system, κ_p is the thermal conductivity of the PCM, κ_m is the thermal conductivity of the gypsum; δ_p is the volume fraction of PCM. The PCM is assumed to be a homogeneous material with negligible temperature gradient inside the material if the thermal resistance inside the microcapsules is lower than the thermal resistance between the PCM and the surroundings.

Thermal diffusivity is another important property in heat transfer as well. It is defined as the thermal conductivity divided by the product of density and specific heat capacity [91]:

$$\alpha = \frac{k}{\rho C_p} \tag{12}$$

where k is the thermal conductivity (W/(m·K)), ρ is the density (kg/m³), and C_p is the specific heat (J/(kg·K)).

Thermal diffusivity can be measured by "the Flash method" as ASTM E1461-07 (Standard Test Method for Thermal Diffusivity by the Flash Method) [92]. In this method, the specimen is placed under a "high intensity short duration radiant energy pulse" as showed in Figure 3.13.

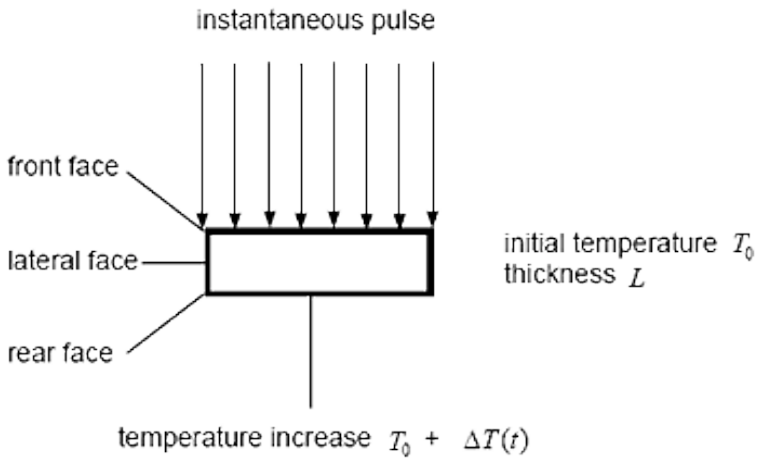

Figure 3.13 Schematic of the flash method [92]

The surface temperature raised by the energy pulse is recorded as function of time (showed as Figure 3.14). Once the temperature is raised to the maximum value, the thermal diffusivity can be calculated from "the half-rise time" and thickness, as:

$$\alpha = \frac{0.13879L^2}{t_{1/2}} \tag{13}$$

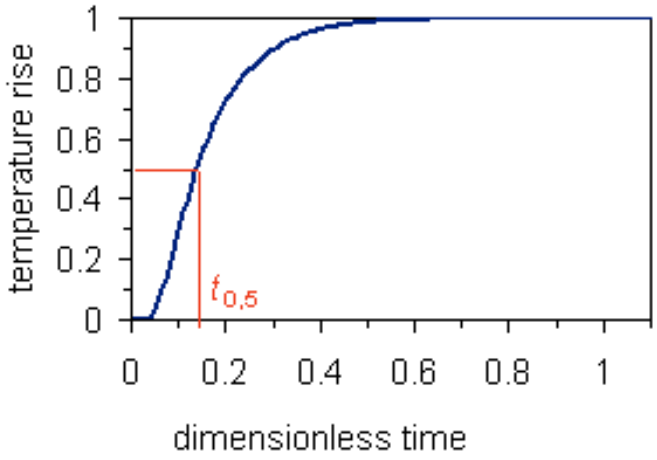

Figure 3.14 Characteristic thermogram for the Flash Method (normalized time and temperature) [92]

The Clemson University Complex and Advanced Materials Laboratory of Dr. Terry Tritt acquired a state-of-the-art Laser flash system to measure thermal diffusivity from which conductivity can be deduced at temperatures ranging from -100°C to 1100°C. However, the system is appropriate for homogeneous dust-free samples, which is not suitable for the plaster/PCM samples. Therefore, a pseudo flash method was devised based on the same principle using a heat lamp as shown in Figure 3.15. The temperatures on both sides of the sample are measured using two type-K thermocouples as functions of time. High temperature high thermal conductivity paste (Omegatherm 201) was applied to reduce the effect of surface roughness and gap conductance between the samples of the thermocouples. Insulation wool was used around the sample in order to reduce the convective heat transfer between the two sides of the sample. The slope of the curve obtained by a given sample is proportional to the conductivity, which can then be

deduced by direct comparison with known samples with appropriate compensation to account for the differences in density and specific heat between samples. The tests were conducted at a temperature greater than the PCM's melting temperature in order to make sure that the latent heat of the PCM does not interfere with the diffusivity measurement.

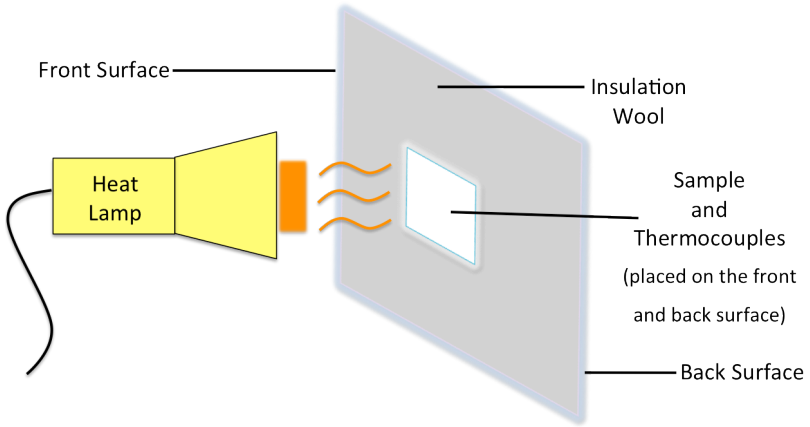

Figure 3.15 Flash method experiment set-up

3.2.2 Micro-scale Characterization

Optical microscopy images were captured on Olympus BX 60 to detect the thermal behavior of the PCM. The PCM was heated to 50°C, 100°C, 150°C, 200°C, 250°C separately at the rate of 10°C/min for an hour before being observed.

The scanning electron microscope (SEM) analysis was performed at room temperature using Hitachi TM-3000 apparatus to study the surface morphology plaster samples integrated with PCM. It is a technique to detect the morphology and size of materials by "scanning the sample with a high-energy beam of electrons" [93]. The electrons interact with the atoms that make up the sample which produces signals "that

contain information about the sample's surface topography, composition, and other properties such as electrical conductivity". This technology is often combined with Energy-dispersive X-ray spectroscopy (EDS) for elemental analysis by detecting characteristic X-ray excitation.

CHAPTER FOUR

RESULTS AND DISCUSSION

Effect of manufacturing process and PCM concentration on the mechanical and thermal properties of plaster boards are discussed by addressing their density, bending strength, and thermal conductivity.

4.1 Effect of PCM on Properties in Different Manufacturing Processes

The industrial manufacturing process of plaster drywall requires curing samples at 260°C for 40 minutes. Since this temperature is fairly high and may degrade most microencapsulated PCMs, other curing processes were considered with lower temperature and longer periods of time even though this may result in loss of productivity. Four different curing processes are considered: (1) Curing the sample at 260°C at the rate of 10°C/min for 40 minutes; (2) Curing the sample at 240°C at the rate of 10°C/min for 50 minutes; (3) Curing the sample at 100°C at the rate of 10°C/min for 3 hours; (4) Curing the sample at 60°C at the rate of 10°C/min for 24 hours. These different curing processes were conducted in order to achieve a balance between desirable properties and productivity.

4.1.1 Effect on Physical Properties

For each sample corresponding to different PCM concentrations and different curing processes, the density (ρ) was calculated using mass and volume, the water

content (u) was calculated using Equation (3) and the porosity (Φ) was calculated using Equation (4). All results are graphed and listed in Figures 4.1 to 4.3 and Tables 4.1 to 4.3.

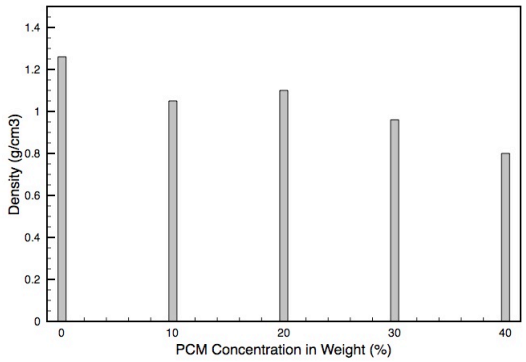

(a) Curing at 260°C for 40 minutes

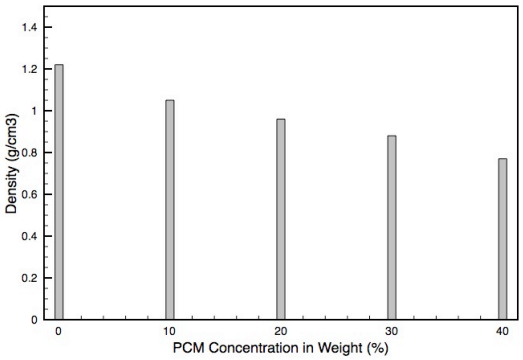

(b) Curing at 240°C for 50 minutes

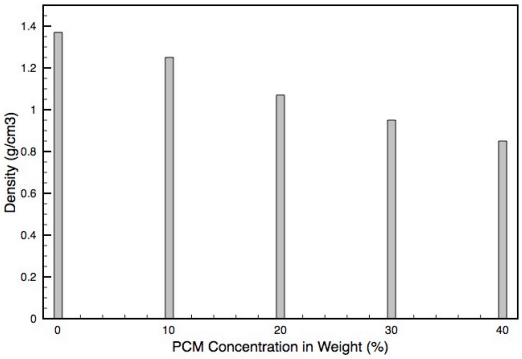

(c) Curing at 100°C for 3 hours

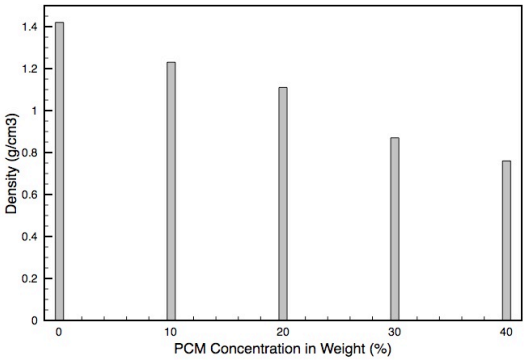

(d) Curing at 60°C for 24 hours

Figure 4.1 Density of plaster samples with different concentration of PCM

Table 4.1 Density of plaster with different concentration of PCM (g/cm3)

Sample #	**1**	**2**	**3**	**4**	**5**
PCM%	**0**	**10**	**20**	**30**	**40**
Process 1: 260°C /40min	1.26	1.05	1.10	0.96	0.80
stdv	*0.17*	*0.03*	*0.14*	*0.09*	*0.21*
Process 2: 240°C /50min	1.22	1.05	0.96	0.88	0.77
stdv	*0.23*	*0.05*	*0.05*	*0.03*	*0.12*
Process 3: 100°C /3h	1.37	1.25	1.07	0.95	0.85
stdv	*0.09*	*0.05*	*0.18*	*0.07*	*0.09*
Process 4: 60°C /24h	1.42	1.23	1.11	0.87	0.76
stdv	*0.09*	*0.03*	*0.05*	*0.02*	*0.03*

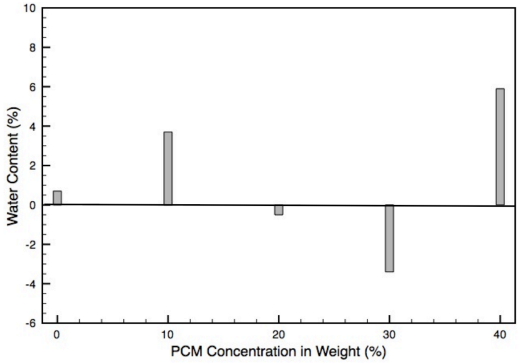

(a) Curing at 260°C for 40 minutes

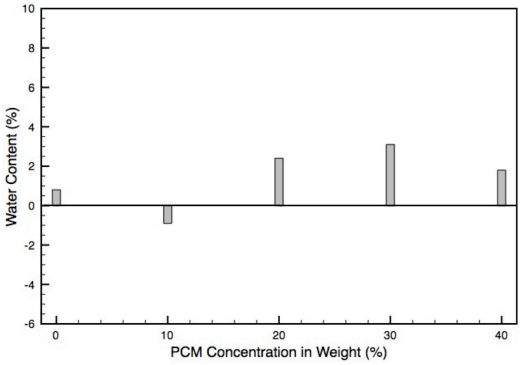

(b) Curing at 240°C for 50 minutes

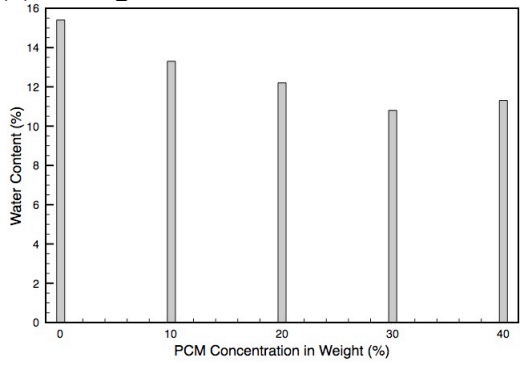

(c) Curing at 100°C for 3 hours

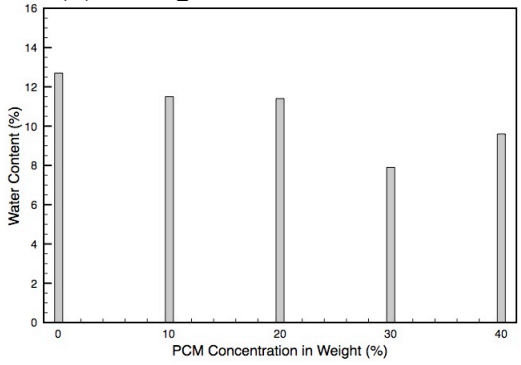

(d) Curing at 60°C for 24 hours

Figure 4.2 Water content of plaster samples with different concentration of PCM

Table 4.2 Water content of plaster samples with different concentration of PCM

Sample #	1	2	3	4	5
PCM%	0	10	20	30	40
Process 1: 260°C/40min	0.7	3.7	-0.5	-3.4	5.9
Process 2: 240°C/50min	0.8	-0.9	2.4	3.1	1.8
Process 3: 100°C/3h	12.7	11.5	11.4	7.9	9.6
Process 4: 60°C/24h	15.4	13.3	12.2	10.8	11.3

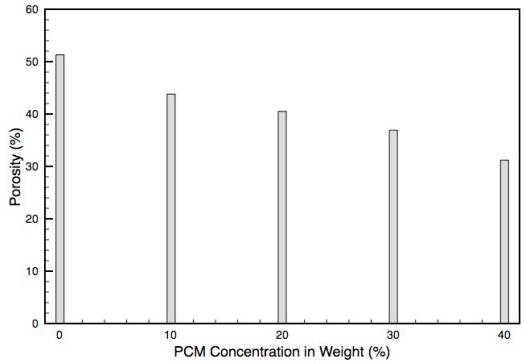

(a) Curing at 260°C for 40 minutes

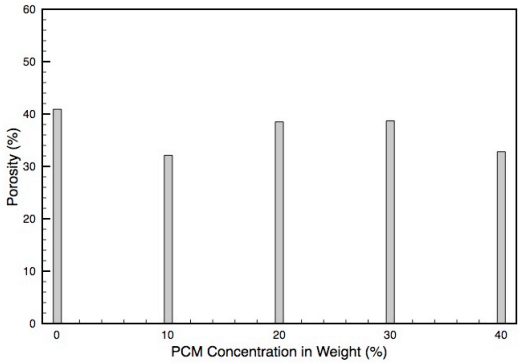

(b) Curing at 240°C for 50 minutes

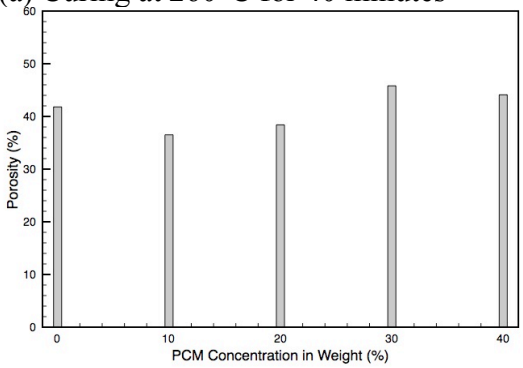

(c) Curing at 100 °C for 3 hours

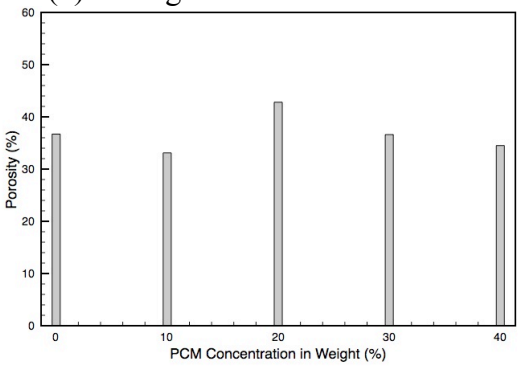

(d) Curing at 60 °C for 24 hours

Figure 4.3 Porosity of plaster with Different Concentration of PCM

Table 4.3 Porosity of plaster with different concentration of PCM

Sample #	**1**	**2**	**3**	**4**	**5**
PCM%	**0**	**10**	**20**	**30**	**40**
Process 1: 260°C/40min	51.3	43.8	40.5	36.9	31.2
Process 2: 240°C/50min	40.9	32.1	38.5	38.7	32.8
Process 3: 100°C/3h	41.8	36.5	38.4	45.8	44.1
Process 4: 60°C/24h	36.7	33.1	42.8	36.6	34.5

Figure 4.1 shows that the density of the plaster samples decreases with increasing PCM concentration. First, this can be explained by the density of PCM ($0.9g/cm^3$) being smaller than that of plaster ($2.32\text{-}2.96g/cm^3$). It indicates that the structure of plaster matrix is changed by the addition of water and PCM, which results in the increase in porosity.

The results of Figure 4.2 (a) and (b) show large differences between PCM percentages. For instance, the water content for 30% and 40% PCM are significantly different even though they are not expected to be that different. This suggests that experimental error should be reduced by increasing the population of samples and tests per sample. Nevertheless, these results are sufficient to capture the difference between curing processes.

Although there is no apparent trend of water content and porosity with increasing PCM concentration (based on Figures 4.2, 4.3 and Tables 4.2, 4.3), it should be noticed that curing the samples at a relatively higher temperature and shorter time yields a lower water content and higher porosity. When the sample was cured at 240°C for 50 minutes,

the water content of the plaster sample with 10% PCM is below 0. This means that the sample lost more water than the amount that was initially added to the hemihydrate. This suggests that a possible process called “inter-conversion” will occur between these structures due to their nearly identical crystal structures, which contain "channels that can accommodate variable amounts of water, or other small molecules". β-anhydrite or "natural" andydrite ($CaSO_4$) which is completely anhydrous forms when the temperature is even higher (above 250°C). These reactions might lead to the different properties of the samples. But since only one set of samples were tested, more measurements are needed to reach statistical significance to conclude these reactions.

4.1.2 Effect on Mechanical Properties

The flexural strength was measured in order to evaluate the mechanical properties of the plaster samples with increasing PCM concentration (0, 10%, 20%, 30% and 40%) in the different curing processes. Two specimens were measured for the same process and each specimen broke after being tested. The broken samples were then prepared to a suitable dimension for the thermal properties measurements.

Results of flexural strength are presented in Table 4.4.

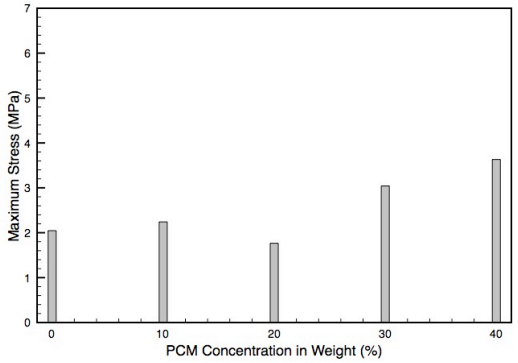

(a) Curing at 260°C for 40 minutes

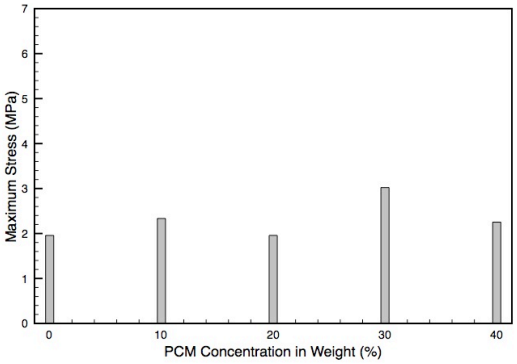

(b) Curing at 240°C for 50 minutes

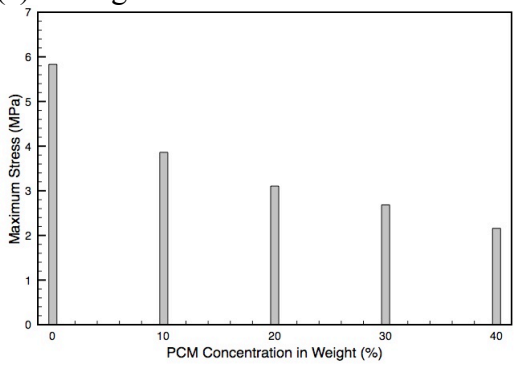

(c) Curing at 100°C for 3 hours

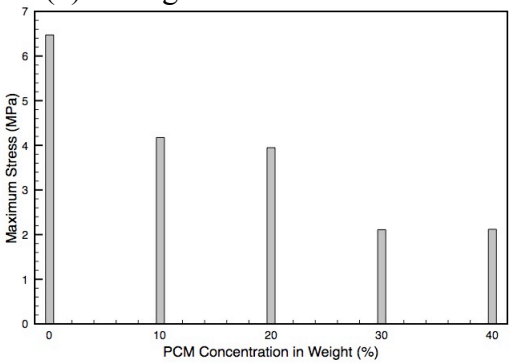

(d) Curing at 60°C for 24 hours

Figure 4.4 Maximum stress of plaster with different concentration of PCM

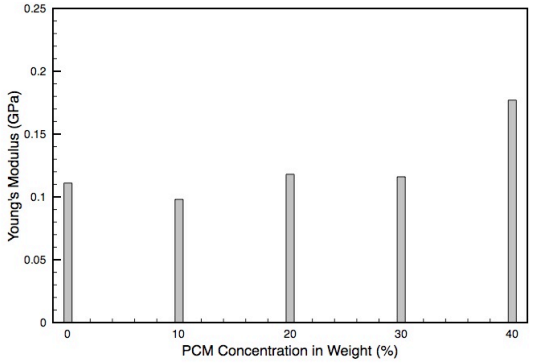

(a) Curing at 260°C for 40 minutes

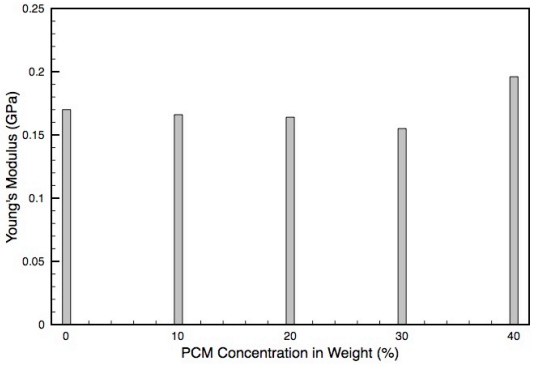

(b) Curing at 240°C for 50 minutes

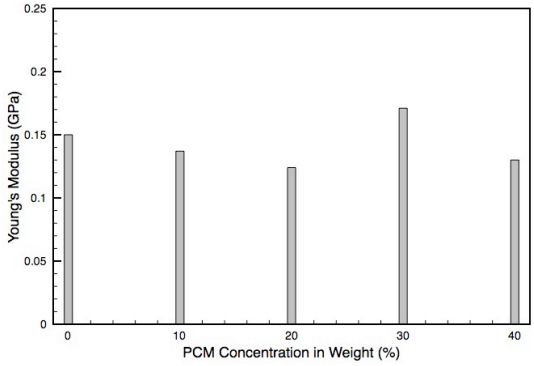

(c) Curing at 100°C for 3 hours

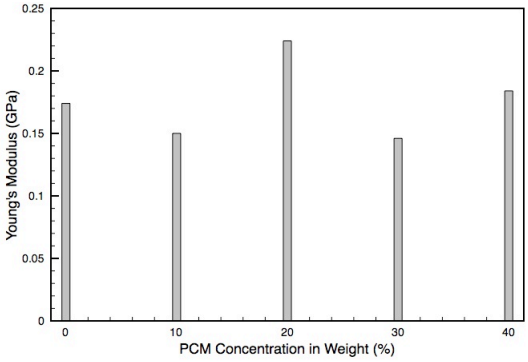

(d) Curing at 60°C for 24 hours

Figure 4.5 Young's modulus of plaster with different concentration of PCM

Table 4.4 Flexural properties of plaster with different concentration of PCM

Process 1: 260°C/40min

Sample #	**1**	**2**	**3**	**4**	**5**
PCM%	**0**	**10**	**20**	**30**	**40**
Maximum Stress (MPa)	2.046	2.241	1.765	3.043	3.632
stdv	*0.723*	*0.998*	*0.205*	*1.289*	*0.072*
Young's modulus(GPa)	0.111	0.098	0.118	0.116	0.177
stdv	*0.067*	*0.048*	*0.072*	*0.070*	*0.151*

Process 2: 240°C/50min

Sample #	**1**	**2**	**3**	**4**	**5**
PCM%	**0**	**10**	**20**	**30**	**40**
Maximum Stress (MPa)	1.956	2.333	1.957	3.021	2.252
stdv	*1.030*	*0.174*	*0.067*	*1.320*	*1.102*
Young's modulus(GPa)	0.170	0.166	0.164	0.155	0.196
stdv	*0.055*	*0.038*	*0.006*	*0.014*	*0.011*

Process 3: 100°C/3h

Sample #	**1**	**2**	**3**	**4**	**5**
PCM%	**0**	**10**	**20**	**30**	**40**
Maximum Stress (MPa)	5.831	3.861	3.104	2.684	2.158
stdv	*2.690*	*2.335*	*0.570*	*0.670*	*0.968*
Young's modulus(GPa)	0.150	0.137	0.124	0.171	0.130
stdv	*0.056*	*0.019*	*0.033*	*0.042*	*0.067*

Process 4: 60°C/24h

Sample #	**1**	**2**	**3**	**4**	**5**
PCM%	**0**	**10**	**20**	**30**	**40**
Maximum Stress (MPa)	6.472	4.174	3.947	2.110	2.119
stdv	*3.128*	*0.694*	*0.223*	*0.090*	*0.219*
Young's modulus (GPa)	0.174	0.150	0.224	0.146	0.184
stdv	*0.077*	*0.005*	*0.023*	*0.032*	*0.006*

The results vary significantly due to the inaccuracy of the equipment and the uncertain nature of brittle fracture. However, based on the measurements, the same trend can be observed in each repeated experiment. From Figures 4.4, 4.5 and Table 4.5, It can be noticed that the stress of the gypsum board sample without PCM is significantly lower when cured at 260°C for 40 minutes and 240°C for 50 minutes than cured at relatively lower temperature (100°C and 60°C). These results correlate with the results of the water content measurement. The results indicate that when the samples are cured at a higher temperature, there is more water evaporated and less water retained which led to the reduction in mechanical properties. The possible reason is the reverse reaction and dehydration reaction may prevent hydration, which is the most important reaction for the development of strength.

Also from the given data different trends can be observed for different curing processes. It suggests that when the samples were cured at 260°C for 40 minutes, the maximum stress decreased with the first introduction of PCM but then increases with the addition of PCM continuously. When the samples were cured at 240°C for 50 minutes, the concentration of PCM did not have significant influence on the stress and Young's modulus of the samples. When the samples were cured at 100°C for 3 hours or 60°C for 24 hours, the addition of PCM particles results in a decrease in maximum stress. No apparent trend was observed for Young's modulus for these two processes. These results show that both the concentration of PCM and curing processes have some effect on the mechanical properties of the samples by influencing water evaporation.

4.1.3 Effect on Thermal Properties

The thermal conductivity of the standard plaster sample and samples with 10%, 20%, 30%, and 40% PCM in different curing process was measured in order to evaluate the thermal properties. Two or three samples were prepared for each curing process and five repeated tests were conducted on each sample. The normalized results are presented in Figure 4.6 and Table 4.5.

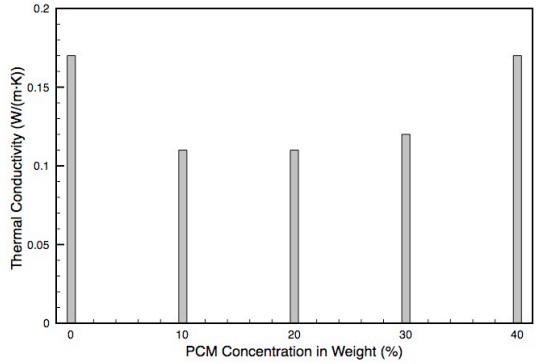

(a) Curing at 260°C for 40 minutes

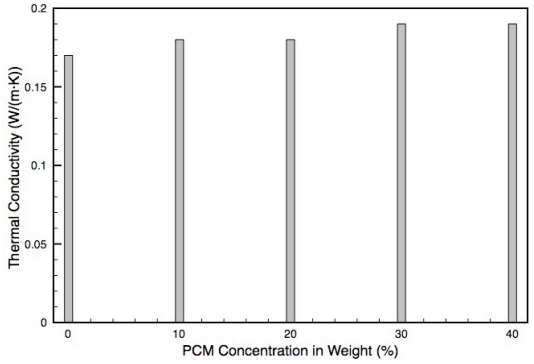

(b) Curing at 240°C for 50 minutes

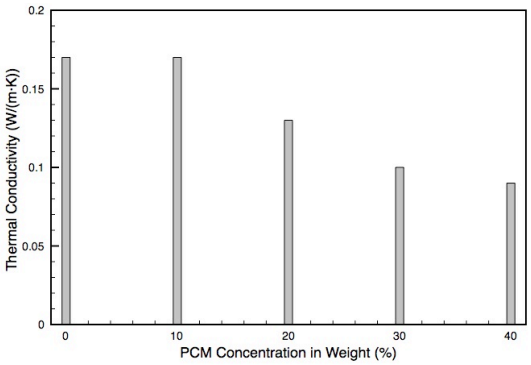

(c) Curing at 100°C for 3 hours

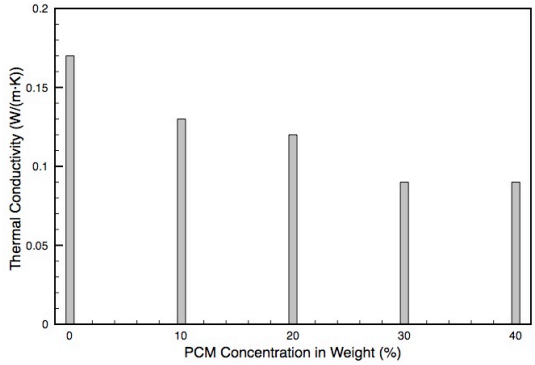

(d) Curing at 60°C for 24 hours

Figure 4.6 Thermal conductivity of plaster with different concentration of PCM

Table 4.5 Thermal conductivity of plaster with different concentration of PCM (W/(m·K))

Sample #	**1**	**2**	**3**	**4**	**5**
PCM%	**0**	**10**	**20**	**30**	**40**
Process 1: 260°C/40min	0.170	0.107	0.115	0.117	0.168
stdv	*0.063*	*0.018*	*0.012*	*0.015*	*0.034*
Process 2: 240°C/50min	0.170	0.180	0.178	0.190	0.186
stdv	*0.000*	*0.009*	*0.005*	*0.000*	*0.031*
Process 3: 100°C/3h	0.170	0.166	0.127	0.099	0.085
stdv	*0.026*	*0.036*	*0.032*	*0.015*	*0.022*
Process 4: 60°C/24h	0.170	0.131	0.119	0.089	0.093
stdv	*0.027*	*0.012*	*0.013*	*0.013*	*0.001*

The results indicate that when the samples were cured at 260°C for 40 minutes, the thermal conductivity increased with the addition of PCM. When the samples were cured at 240°C for 50 minutes, the concentration of PCM does not have significant influence on the thermal conductivity of the samples. When the samples were cured at 100°C for 3 hours or 60°C for 24 hours, the addition of PCM particles results in a decrease of thermal conductivity.

The thermal conductivity of the samples can be predicted by Maxwell's relation (Eq. (9)) as a theoretical check. This model calculates the effective conductivity of a mixture based on two conductivity values and their respective volume fractions. One of the conductivity values is that of gypsum (0.17 W/(m.K)) and the other should be that of the PCM. Since the PCM is made of micro-capsules composed of two materials (i.e., the

hexadecane core and the Melamine-urea-formaldehyde shell), the conductivity of the PCM is a value between that of these two materials. Therefore the effective conductivity of the mixture can be estimated by considering either the thermal conductivity of the core material or that of the polymer shell. It is reported in the literature [79] that while the heat capacity microencapsulated PCM is more related to the core material, the thermal conductivity depends significantly on the chemical composition of the polymer shell. Thermal conductivity of Hexadecane (0.16 W/(m·K)) is reported to be higher than that of Melamine-urea-formaldehyde (0.04 W/(m·K)). The predicted results are showed as Table 4.6. Note that Maxwell's model accountS for the volume fraction of the different constituents of the mixture and does not account for the effects of the curing process. Therefore, the experimental results show the limitations of Maxwell's model.

Table 4.6 Thermal conductivity predicted by Maxwell's relation (W/(m·K))

Sample #	**1**	**2**	**3**	**4**	**5**
PCM%	**0**	**10**	**20**	**30**	**40**
Using hexadecane's conductivity	0.170	0.167	0.164	0.161	0.159
Using MUF's conductivity*	0.170	0.144	0.123	0.106	0.092

*MUF: Melamine-urea-formaldehyde

With increasing PCM concentration, the thermal conductivity predicted by Maxwell's model has the opposite trend of that of the measured thermal conductivity of the samples cured at high temperature. One of the possible reasons is the potential rupture of the polymer shell at high temperature and leakage of the hexadecane throughout the gypsum matrix. The interaction between the hexadecane (which has a higher conductivity) and the gypsum may increase the overall conductivity of the mixture. At

low curing temperatures, the conductivity of the mixture seems to be governed by the shell's conductivity (which is lower) which would explain why Maxwell's model and the experimental results follow the same trend with increasing PCM concentration.

The results of thermal diffusivity measurement using the flash method are shown in Figure 4.7 as the difference between temperatures at the front and back of the samples. The plaster samples with 0%, 10% and 40% PCM in weight were cured at 260°C for 40 minutes and 60°C for 24 hours. Two specimens of each sample were tested and three measurements were taken for each specimen. These results were adjusted to account for the differences in thickness of the samples [92].

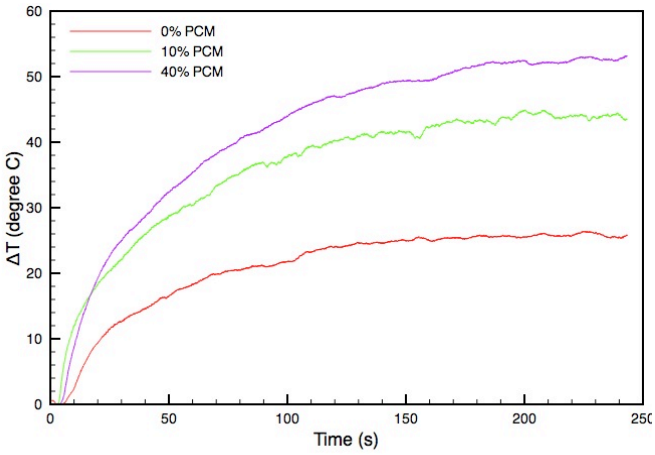

(a) Curing at 260°C for 40 minutes

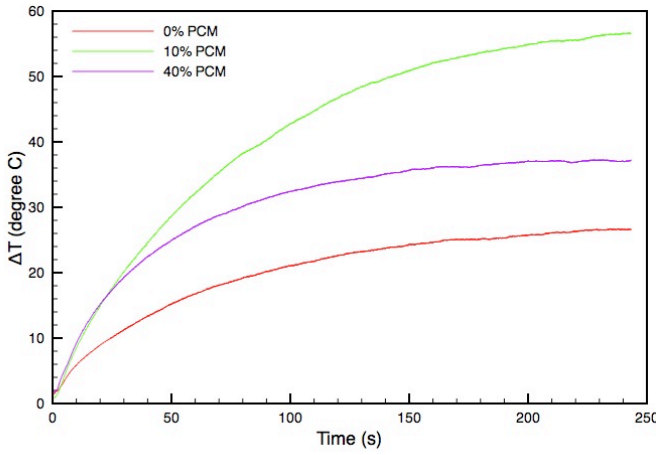

(b) Curing at 60°C for 24 hours

Figure 4.7 Thermal diffusivity measurements of gypsum-PCM samples

It can be observed that when the samples were cured at 260°C for 40 minutes, the slope of the samples with 40% PCM is higher than with 10% PCM, and the slope of the samples with 10% PCM is higher than with no PCM. When the samples were cured at 60°C for 24 hours, the slope of the plaster samples with 40% PCM is higher than with no PCM, and the slope of the plaster samples with 10% PCM is higher than with 40% PCM. The curves of the samples with no PCM made by these two processes agree well with each other.

As a higher thermal diffusivity means the samples can adjust its temperature to its surroundings faster, adding PCM will speed the heat conduction and require less energy compared with their "volumetric heat capacity" [92]. Based on the experimental study, the density greatly decreases as the PCM concentration increases. And according to some research [51], the specific heat increases with increasing concentration of PCM, but since all the samples are tested at the same temperature (which is above the PCM's melting temperature), the effect of the two curing processes on specific heat can be neglected.

However, the different curing processes leads to a different trend in thermal conductivity. For the samples cured at 260°C for 40 minutes, thermal conductivity first decreased with increasing PCM concentration and then increases with PCM concentration. For the samples cured at 60°C for 24 hours, the trend is different. The thermal conductivity decreases with increasing PCM concentration. These results confirm the experimental results obtained using the thermal pile experiment of the previous section.

4.1.4 Possible Mechanisms

The effect of the heating processes on the microencapsulated PCM was studied using microscope inspection. The PCM for analysis was heated to a certain temperature ranging from 50°C to 250°C and then it was observed under the microscope. The microscope images are shown in Figure 4.8.

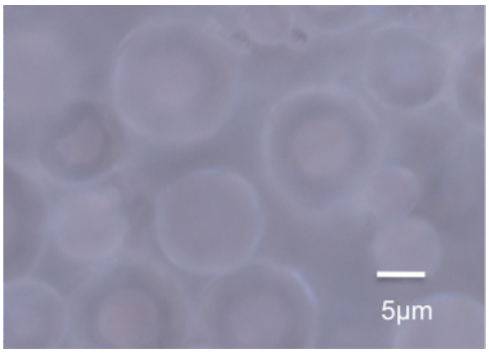

(a) 50°C

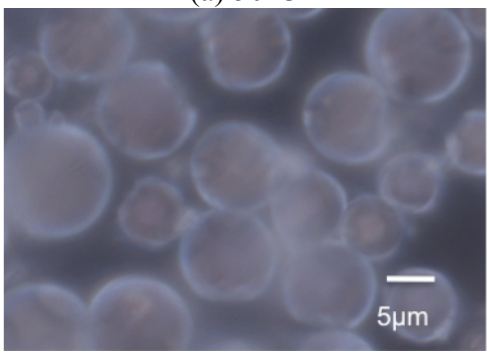

(b) 100°C

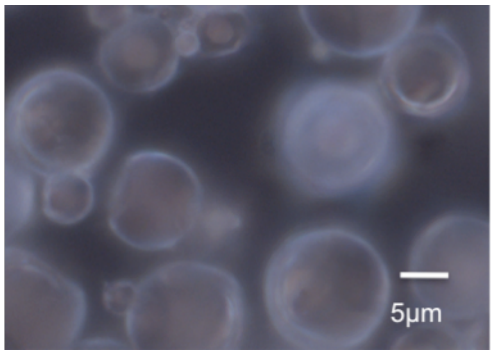

(c) 150°C

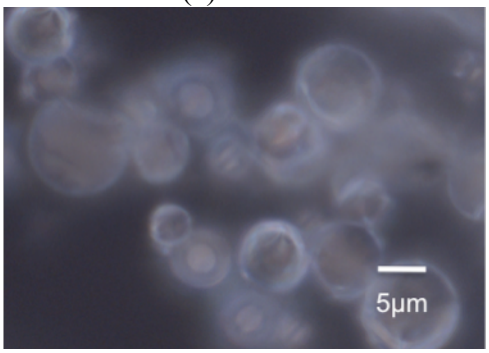

(d) 200°C

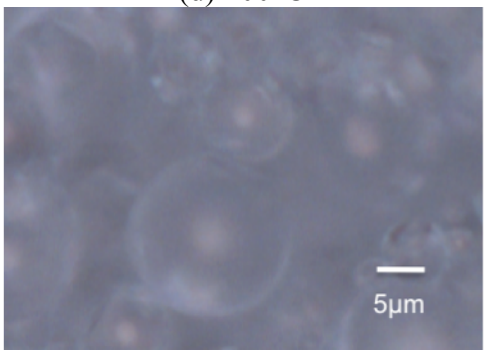

(e) 250°C

Figure 4.8 Optical micrographs of Microtek 18D PCM at different temperatures. As the temperature increases, the particles become increasingly distorded and agglomerated.

The structure of the capsules is observed to be stable when the samples are heated to a temperature lower than 100°C. When the samples are heated to a temperature above 150°C, the shell of the microspheres begins to deform and eventually rupture. Above

200°C, the micro-capsules appear to be damaged and agglomerated to a large extent. As the samples are heated at 250°C, the destroyed polymer shells can be observed.

To further understand the mechanism of how PCM interact with plaster matrix and influence the mechanical and thermal properties, standard sample and plaster sample with 10% and 40% PCM cured at 260°C for 40 minutes ware examined by optical and scanning electron microscopy (SEM) to visually characterize the microstructure, bond region topography, and porosity. Energy dispersive x-ray spectroscopy (EDS) was applied to gather information about the chemical composition of different points. Plaster samples with 0%, 10% and 40% PCM cured at 260°C for 40 minutes were observed. The SEM images are showed in Figure 4.9.

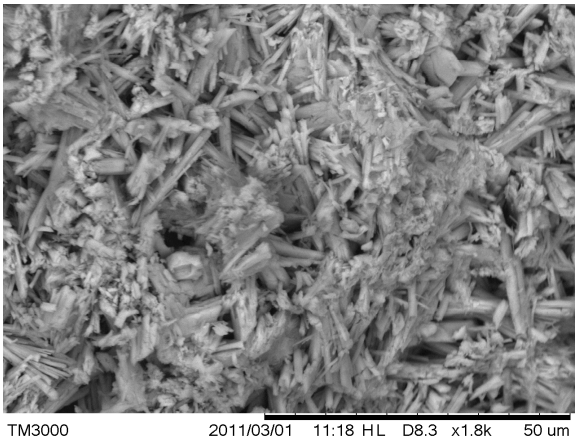

(a) Reference Mixture

(b) 10% PCM Mix

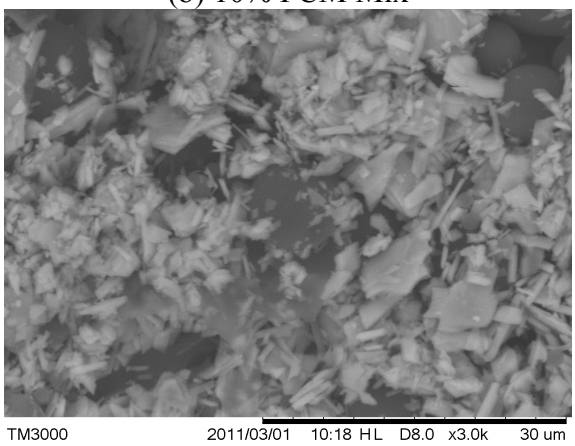

(c) 40% PCM Mix

Figure 4.9 SEM micrographs of gypsum-PCM samples. The particles of PCM (dark rounded regions) are dispersed within the particles of gypsum (lighter shade), sometimes fill voids and are damaged (such as seen in (b)).

The SEM analysis shows a porous micro-structure of the plaster sample (white particles) with the microencapsulated PCM (sphere and darker spaces). As paraffin has a low melting temperature of 18°C, it melts earlier than the polymer shell during the heating process. It can be assumed that this segregation could cause solidification at the cavity and pores of the plaster matrix due to the immiscibility between the PCM and the plaster matrix [52], which result in the change of the mechanical and thermal properties.

The SEM suggests that there is leakage of the paraffin and the shell is damaged to some extent.

The elemental composition of PCM in different parts of the plaster sample with 0, 10%, and 40% PCM was determined by energy dispersive X-ray analysis (EDS). Three scans were taken and analyzed for each of the three samples. The points are selected at the plaster particles, sphere PCM particles, dark spaces, and the boundary where PCM and plaster particles contact with each other. EDS analysis results are provided in Figure 4.10.

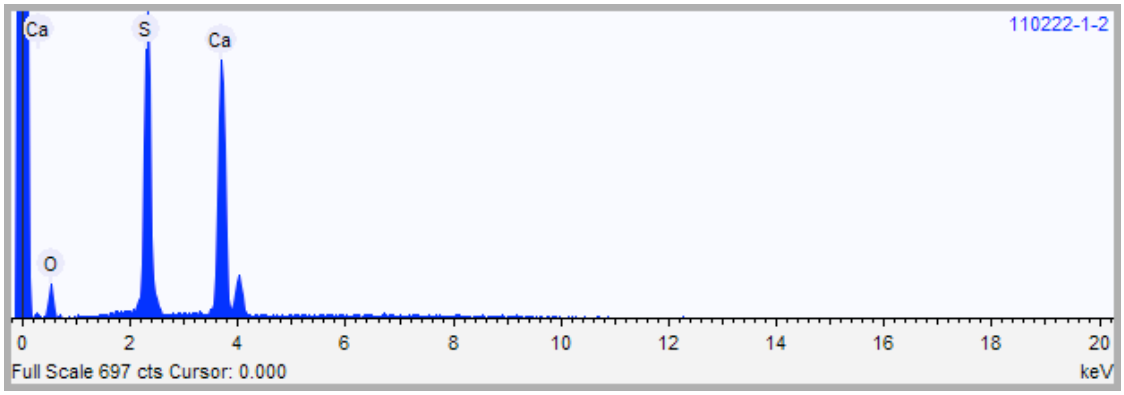

(a) Reference Mixture

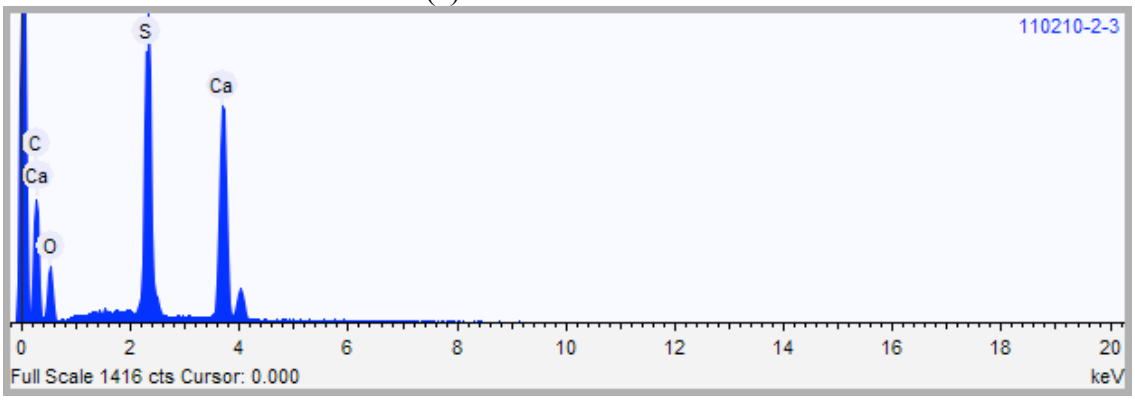

(b) 10% PCM Mix

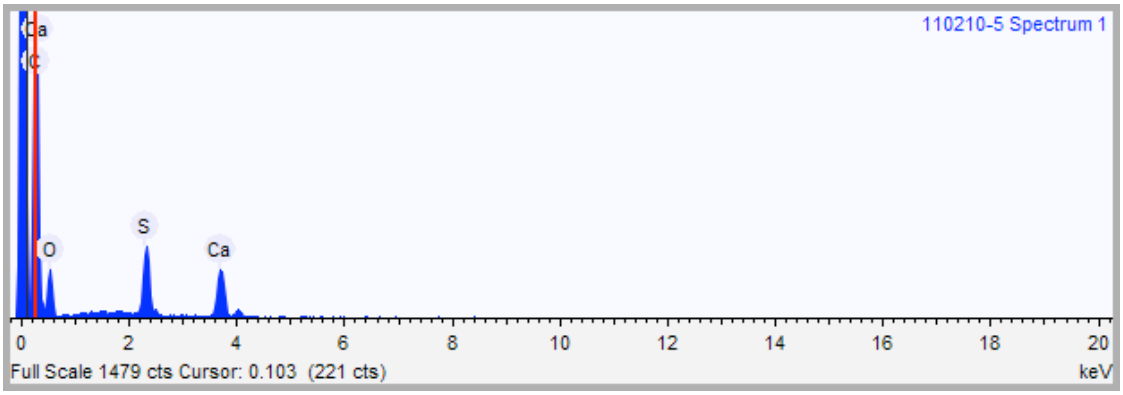

(c) 40% PCM Mix

Figure 4.10 EDS Spectra of plaster samples with different concentration of PCM

In the plaster sample without PCM, the main composition is Calcium, Oxygen, and Sulfur as expected. The level of Carbon of plaster sample with 10% PCM varies from 22.9 to 49.0% in weight at different point compared with the level of Calcium from 15.1% to 25.2%. When the content of PCM is increased to 40%, the level of Carbon is further increased, which ranges from 53.9% to 68.1%, against 5.9 to 10.3% of Calcium. The distinct peak of Carbon is due to the presence of PCM, and the level of Carbon increases with the addition of PCM. These results indicate that PCM interacted and formed a complex with the plaster particles that changed the structure of plaster at this temperature.

These results show that both the PCM particles and curing process both have some effects on the mechanical properties of the samples by influencing the water evaporation process.

4.2 Effect of Aluminum Powder in Controlling Thermal Conductivity

Low thermal conductivity may result in slower charging and discharging time which may limit the use of PCM. Aluminum particles have been reported to improve the thermal conductivity in several publications since they have an obviously higher thermal conductivity than PCM and plaster [33, 34]. In order to control the thermal conductivity, Aluminum powder is introduced in the plaster samples with 40% PCM in contrast with plaster samples with no PCM and 40% PCM. Because the temperatures of 260°C and 240°C are too high for the mixture system, the samples were only cured at 60°C for 3h or 100°C for 24h for safety reasons. Then the density, flexural strength, and thermal conductivity of the samples were measured.

The density of the samples was measured and reported in Figure 4.11.

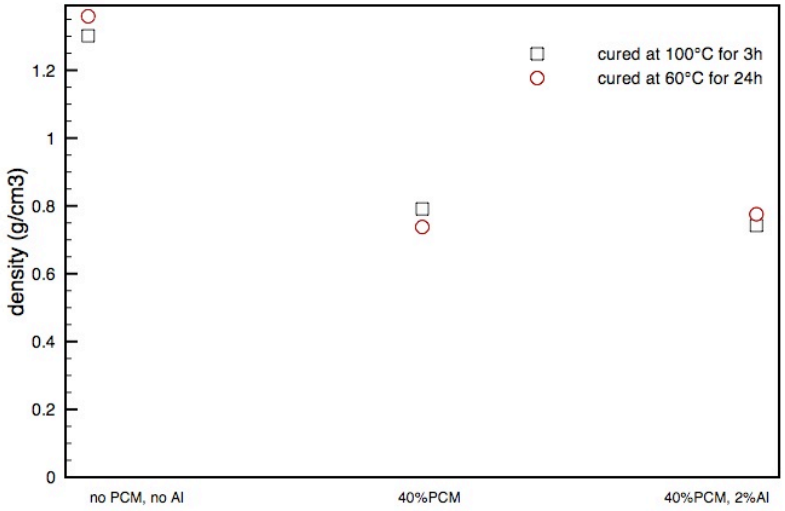

Figure 4.11 Density of plaster samples with Aluminum powder

Table 4.7 Density of plaster with Aluminum powder (g/cm3)

Sample #	1	2	3
PCM%	0	40	40
Al%	0	0	2
Process 1: 100°C/3h	1.30	0.79	0.74
Process 2: 60°C/24h	1.36	0.74	0.78

Then the bending strength of the samples was measured by the same instrument. The results of maximum stress (MPa) and Young's Modulus (GPa) are given as Figure 4.12 and Figure 4.13 below.

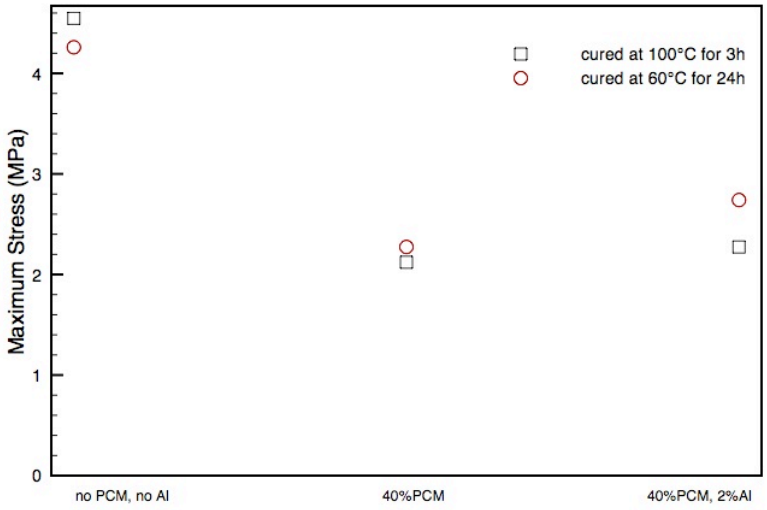

Figure 4.12 Maximum stress of plaster samples with Aluminum powder

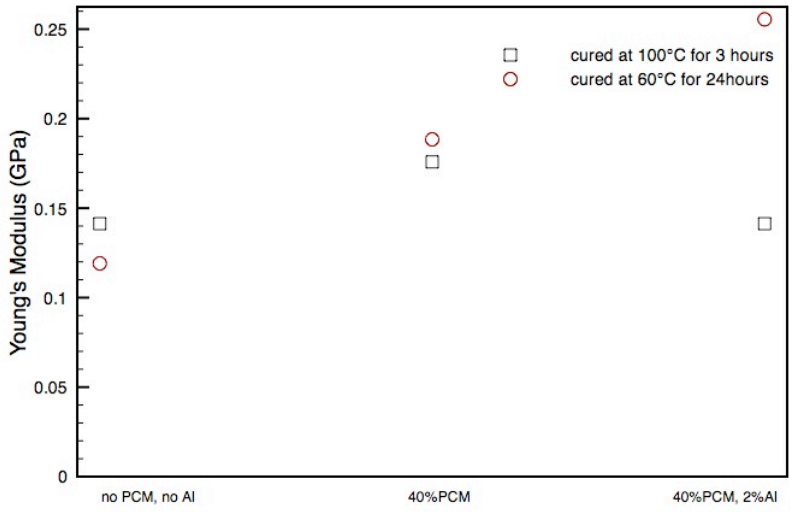

Figure 4.13 Young's modulus of plaster with Aluminum powder

Table 4.8 Flexural properties of plaster with Aluminum powder

Process 1: 100°C/3h

Sample #	**1**	**2**	**3**
PCM%	**0**	**40**	**40**
Al%	**0**	**0**	**2**
Break Force (lb)	30.00	14.00	15.00
Break Force (N)	133.45	62.28	66.72
Maximum Stress (MPa)	4.55	2.12	2.28
Maximum Strain	0.032	0.012	0.016
Young's modulus(GPa)	0.141	0.176	0.141

Process 2: 60°C/24h

Sample #	1	2	3
PCM%	0	40	40
Al%	0	0	2
Break Force (lb)	34.00	15.00	14.00
Break Force (N)	151.24	66.72	62.28
Maximum Stress (MPa)	4.26	2.27	2.74
Maximum Strain	0.036	0.012	0.011
Young's modulus(GPa)	0.119	0.188	0.255

The thermal conductivity of the standard plaster sample and the samples with 2% Aluminum powder and 40% PCM was measured to compare with the thermal conductivity of the plaster samples with 40% PCM without Aluminum powder in order to evaluate the effect of Aluminum powder on thermal properties (Figure 3.14).

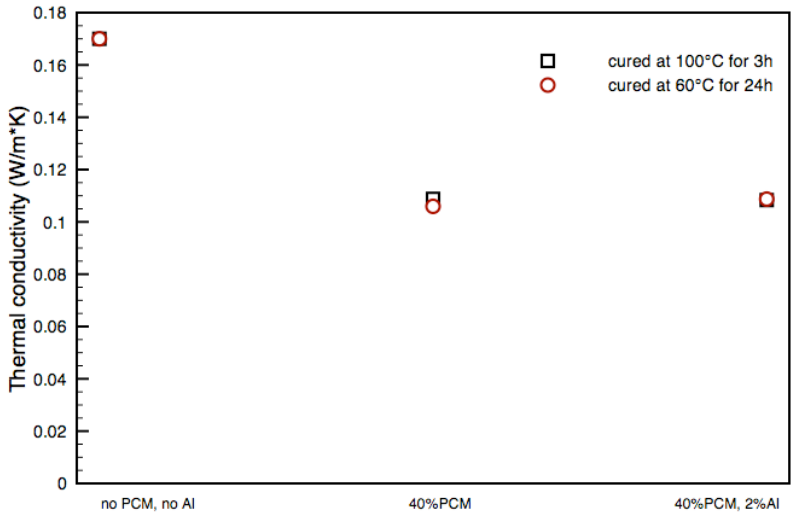

Figure 4.14 Thermal conductivity of plaster with Aluminum powder

This result is then compared with the thermal conductivity predicted by Maxwell's relation listed in Table 4.9.

Table 4.9 Thermal conductivity of plaster with Aluminum powder (W/(m·K))

Experimental Result

Sample #	**1**	**2**	**3**
PCM%	**0**	**40**	**40**
Al%	**0**	**0**	**2**
Process 1: 100°C/3h	0.170	0.109	0.108
Process 2: 60°C/24h	0.170	0.106	0.109

Result Predicted by Maxwell's relation

Sample #	**1**	**2**	**3**
PCM%	**0**	**40**	**40**
Al%	**0**	**0**	**2**
core	0.170	0.159	0.169
shell	0.170	0.092	0.098

It can be concluded that the addition of Aluminum powder did not affect the density and the bending strength significantly. Also, it did not have as much influence on increasing the thermal conductivity as expected. This may be due to the low concentration of Aluminum powder. Also, the powder may not disperse uniformly due to its low concentration. Since only one sample is tested for each of the processes, statistical significance should be included by conducting tests on more than one sample. Also, increased concentration of Aluminum powder under safety conditions should be tested and compared in order to achieve the control of the thermal conductivity of the samples.

CHAPTER FIVE

CONCLUSION AND FUTURE WORK

In this research, the first objective is to investigate the physical and thermal properties of various PCMs in order to determine whether they can handle the industrial manufacturing process of gypsum wallboards. The second objective is to evaluate the effect of the concentration of PCM on the physical, thermal and mechanical properties of the gypsum wallboards. The third objective is to study the effect of different curing processes on the properties of the gypsum wallboards.

The experimental study of this research can be summarized as following:

- Studied the curing process of plaster drywall and then investigated the physical and thermal properties of four different types of PCMs available (including Microtek 18D, Microtek 28D, Microtek 37D, Micronal DS5001) to demonstrate their use for these processes by FTIR, Electron Microscope, TGA and DSC, since the industrial manufacturing process requires heating up the system to 260°C.
- Prepared gypsum wallboard samples with 0, 10, 20, 30, and 40% of Microtek 18D in weight using four different curing processes in laboratory scale. The four different curing processes in this research are: (1) Curing the sample at 260°C at the rate of 10°C/min for 40 minutes; (2) Curing the sample at 240°C at the rate of 10°C/min for 50 minutes; (3) Curing the sample at 100°C at the rate of 10°C/min for 3 hours; (4) Curing the sample at 60°C at the rate of 10°C/min for 24 hours.

- Prepared PCM integrated gypsum samples with 2% Aluminum powder. The samples are only prepared by processes (3) and (4) due to safety reasons.
- Developed bending strength and thermal conductivity testing according to modified ASTM standards to evaluate the effect of the PCM and Aluminum powder. Density, flexural strength, and thermal conductivity are measured.
- Used SEM-EDS and Electron Microscope to study the mechanisms at the micro-scale level.

The main conclusions of this research include:

- Only Microtek 18D is found to be thermally stable to the temperature generally used in the commercial curing process (i.e., 260^{o}C). Other PCMs lose more than 5% of their weight when heated to 260 °C, which means that they cannot be used in the typical manufacturing process. Exothermic peaks of PCM can be observed at 34.14 °C and around 200°C, which refer to the melting behavior of the paraffin core and the polymerization of the polymer shell separately. The encapsulation of the PCM is suspected to prevent it from catching on fire easily when heated to a temperature that is above the flash point of hexadecane.
- The density decreases with increasing concentration of PCM due to the lower density of PCM and the added porosity of the mixture.
- The manufacturing process seems to affect the bending strength and the thermal conductivity significantly based on the limited experimental data:
    - when the samples are cured at 260°C for 40 minutes, the strength seems to decrease with the first introduction of PCM and then increases with the

addition of PCM continuously. The thermal conductivity seems to increase with the addition of PCM.

- when the samples are cured at 240°C for 50 minutes, the concentration of PCM does not have significant influence on the strength and thermal conductivity of the samples according to the measurements.
- when the samples are cured at 100°C for 3 hours or 60°C for 24 hours, the addition of PCM particles results in a decrease of the strength and thermal conductivity.
- the strength of the gypsum board samples without PCM is significantly lower when cured at 260°C for 40 minutes and 240°C for 50 minutes than cured at relatively lower temperature.

- Aluminum powder is not detected to have much impact on the overall properties due to its low concentration.

PCM is suspected to experience rupture and leakage at temperature higher than 200°C. Also, PCM is detected to agglomerate and interact with plaster particles according to the SEM and EDS results. The hydration reaction, which plays an important role in developing mechanical and thermal properties, is suspected to be influenced by the manufacturing process. These processes may lead to the change in the physical and thermal properties of the samples.

Based on these results, the following work is suggested to be done in the future. Firstly, more reliable instruments are needed to improve the accuracy of the results. Secondly, more repeated experiments are needed to reach statistically significant results.

Thirdly, different concentration of Aluminum powder and other additives need to be studied in controlling the properties of the samples.

REFERENCES

1. N. Zhu, Z. Ma, S. Wang, "Dynamic characteristics and energy performance of buildings using phase change materials: A review", *Energy Conversion and Management*, Vol. 50: 3169–3181, 2009.

2. A. Sharma, V.V. Tyagi, C.R. Chen, D. Buddhi, "Review on thermal energy storage with phase change materials and applications", *Renewable and Sustainable Energy Reviews*, Vol. 13: 318–345, 2009.

3. V.V. Tyagi, S.C. Kaushik, S.K. Tyagi, T. Akiyama, "Development of phase change materials based on micro-encapsulated technology for buildings: a review", *Renewable and* Sustainable Energy Reviews, Vol.15: 1373–1391, 2011.

4. A. M. Khudhair, M. M. Farid, "A review on energy conservation in building applications with thermal storage by latent heat using phase change materials", *Energy Conversion and Management*, Vol. 45: 263-275, 2004.

5. M. M. Farid, A. M. Khudhair, S. Razack, S. Al-Hallaj, "A review on phase change energy storage: materials and applications", *Energy Conversion and Management*, Vol. 45: 1597–1615, 2004.

6. V.V. Tyagi, S.C. Kaushik, S.K. Tyagi, T. Akiyama, "Development of phase change materials based on micro-encapsulated technology for buildings: a review", *Renewable and* Sustainable Energy Reviews, Vol.15: 1373–1391, 2011.

7. A. M. Khudhair, M. M. Farid, "A review on energy conservation in building applications with thermal storage by latent heat using phase change materials", Energy Conversion and Management, Vol. 45: 263-275, 2004.

8. Kosny, J., D. Gawin, and A. Desjarlais. 2001. "Energy benefits of application of massive walls in residential buildings." *DOE, ASHRAE, ORNL Conference—Thermal Envelopes VIII*, Clear Water, Florida, December 2001.

9. R. Baetensa, B Jelle, A. Gustavsend, "Phase change materials for building applications: A state-of-the-art review", *Energy and Buildings*, Vol. 42: 1361–1368, 2010.

10. M. Telkes, Nucleation of super saturated inorganic salt solution, *Indust Eng Chem*, Vol. 44:1308, 1952.

11. M. Telkes, “Thermal storage for solar heating and cooling”, *Proceedings of the Workshop on Solar Energy storage Subsystems for the Heating and Cooling of Buildings*, Charlottesville, VA, USA, 1975.

12. M. Kenisarin_, K. Mahkamov, “Solar energy storage using phase change materials”, *Renewable and Sustainable Energy*, Vol. 11: 1913–1965, 2007

13. A Sarı, “Thermal reliability test of some fatty acids as PCMs used for solar thermal latent heat storage applications”, *Energy Conversion and Management*, Vol. 44: 2277–2287, 2003

14. American Society of Heating, Refrigerating and Air-Conditioning Engineers, URL: http://www.ashrae.org/, Accessed on Nov 29, 2011.

15. M.F. Demirbas, Thermal energy storage and phase changing materials: an overview, *Energy Resources, Part B: Economics, Planning and Policy*, Vol. 1 (1): 85–95, 2006.

16. J. Dieckmann, “Latent heat storage in concrete”, Technische Universität Kaiserslautern, Kaiserslautern, Germany. http://www.eurosolar.org, 2008 (retrieved 09.12.08).

17. M. M. Kenisarin, “High-temperature phase change materials for thermal energy storage”, *Renewable and Sustainable Energy*, Vol. 14: 955–970, 2010.

18. Y. Cai, Y. Hua, S. Lei, H. Lu, Z. Chen, W. Fan, “Preparation and characterizations of HDPE–EVA alloy/OMT nanocomposites/paraffin compounds as a shape stabilized phase change thermal energy storage material”, *Thermochimica Acta*, Vol. 451: 44–51, 2006.

19. Y. Cai, Q. Wei, F. Huang, S. Lin, F. Chen, W. Gao, “Thermal stability, latent heat and flame retardant properties of the thermal energy storage phase change materials based on paraffin/high density polyethylene composites”, *Renewable Energy*, Vol. 34: 2117–2123, 2009.

20. Y. Cai, Y. Hu, L. Song, Q. Kong, R. Yang, Y. Zhang, Z. Chen, W. Fan, “Preparation and flammability of high density polyethylene/paraffin/organophilic montmorillonite hybrids as a form stable phase change material”, *Energy Conversion and Management*, Vol. 48: 462–469, 2007.

21. Y. Hong, X. Ge, “Preparation of polyethylene paraffin compound as a form stable solid-liquid phase change material,” *Solar Energy Material and Solar Cells*, Vol. 64: 37-44, 2000.

22. A. Karaipekli, A. Sari, K. Kaygusuz, “Thermal conductivity improvement of stearic acid using expanded graphite and carbon fiber for energy storage applications”, *Renewable Energy*, Vol. 32: 2201–2210, 2007.

23. A. Karaipekli, A. Sari, “Capric–myristic acid/expanded perlite composite as form-stable phase change material for latent heat thermal energy storage”, *Renewable Energy*, Vol. 33: 2599– 2605, 2008.

24. A. Karaipekli, A. Sari, “Capric–myristic acid/vermiculite composite as form-stable phase change material for thermal energy storage”, *Solar Energy*, Vol. 83: 323–332, 2009.

25. A. Sari, A. Karaipekli, “Thermal conductivity and latent heat thermal energy storage characteristics of paraffin/expanded graphite composite as phase change material”, *Applied Thermal Engineering*, Vol. 27: 1271–1277, 2007.

26. A. Sari, A. Karaipekli, “Preparation and thermal properties of capric acid/palmitic acid eutectic mixture as a phase change energy storage material”, *Materials Letters*, Vol. 62: 903–906: 2008.

27. A. Sari, A. Karaipekli, “Preparation, thermal properties and thermal reliability of capric acid/expanded perlite composite for thermal energy storage”, *Materials Chemistry and Physics*, Vol. 109: 459–464, 2008.

28. A. Sari, A. Karaipekli, “Synthesis, characterization, thermal properties of a series of stearic acid esters as novel solid–liquid phase change materials”, *Materials Letters*, Vol. 63: 1213–1216, 2009.

29. A. Sari, C. Alkan, A. Karaipekli, O. Uzun, “Microencapsulated n-octacosane as phase change material for thermal energy storage”, *Solar Energy*, Vol. 83: 1757–1763, 2009.

30. A. Sari, C. Alkan, A. Karaipekli, “Preparation, characterization and thermal properties of PMMA/n-heptadecane microcapsules as novel solid–liquid microPCM for thermal energy storage”, *Applied Energy*, Vol. 87: 1529–1534, 2010.

31. C. Alkan, A. Sari, A. Karaipekli, O. Uzun, “Preparation, characterization, and thermal properties of microencapsulated phase change material for thermal energy storage”, *Solar Energy Materials & Solar Cells*, Vol: 93: 143–147, 2009.

32. L. Wang, D. Meng, “Fatty acid eutectic/polymethyl methacrylate composite as form-stable phase change material for thermal energy storage”, *Applied Energy*, Vol. 87 (8): 2660-2665, 2010.

33. W. Wang, X. Yang, Y. Fang, J. Ding, J. Yan, “Preparation and thermal properties of polyethylene glycol/expanded graphite blends for energy storage”, *Applied Energy*, Vol. 86: 1479–1483, 2009.

34. W. Wang, X. Yang, Y. Fang, J. Ding, “Preparation and performance of form-stable polyethylene glycol/silicon dioxide composites as solid–liquid phase change materials”, *Applied Energy*, Vol. 86: 170–174, 2009.

35. X. Liu, H. Liu, S. Wang, L. Zhang, H. Cheng, “Preparation and thermal properties of form stable paraffin phase change material encapsulation,” *Solar Energy*, Vol. 80: 1561-1567, 2006.

36. Y. Zhang, J. Ding, X. Wang, R. Yang, K. Lin, “Influence of additives on thermal conductivity of shape-stabilized phase change material”, *Solar Energy Materials & Solar Cells*, Vol. 90: 1692–1702, 2006.

37. Y. Zhang, K. Lin, R. Yang, H. Di, Y. Jiang, “Preparation, thermal performance and application of shape-stabilized PCM in energy efficient buildings”, *Energy and Buildings*, Vol. 38: 1262–1269, 2006.

38. R. Yang, Y. Zhang, X. Wang, Y. Zhang, Q. Zhang , “Preparation of n-tetradecane-containing microcapsules with different shell materials by phase separation method”, *Solar Energy Materials & Solar Cells*, Vol. 93:1817–1822, 2009.

39. M. Ahmad, A. Bontemps, H. Sallee, D. Quenard, “Experimental investigation and computer simulation of thermal behaviour of wallboards containing a phase change material”, *Energy and Buildings*, Vol. 38: 357–366, 2006.

40. M. Ahmad, A. Bontemps, H. Sallee, D. Quenard, “Thermal testing and numerical simulation of a prototype cell using light wallboards coupling vacuum isolation panels and phase change material”, *Energy and Buildings* Vol. 38: 673–681, 2006.

41. H. Manz, P. W. Egolf, P. Suter and A. Goetzberger, “Tim–PCM External Wall System For Solar Space Heating and Daylighting”, *Solar Energy*, Vol. 61 (6): 369–379, 1997.

42. A.K. Athenitis, C. Liu , D. Hawes, D. Banu, D. Feldman, “Investigation of the Thermal performance of a passive solar test room with wall latent heat storage,” *Build Environ.*,Vol.32: 405-10, 1997.

43. C. Chen, H. Guo , Y. Liu, Hailin Yue[a] and Chendong Wang, "A new kind of phase change material (PCM) for energy-storing wallboard", *Energy and Buildings*, Vol. 40 (5): 882-890, 2008.

44. D. Heim, J. A. Clarke, "Numerical modelling and thermal simulation of PCM–gypsum composites with ESP-r", *Energy and Buildings*, Vol. 36: 795–805, 2004.

45. A. M. Borreguero, M. L. Sánchez, J. L. Valverde, M. Carmona, J. F. Rodríguez, "Thermal testing and numerical simulation of gypsum wallboards incorporated with different PCMs content", *Applied Energy*, Vol. 88: 930–937, 2001.

46. K. Darkwa, P.W. O_Callaghan, D. Tetlow, "Phase-change drywalls in a passive-solar building", *Applied Energy*, Vol. 83: 425–435, 2006.

47. Q. Yan, L. Chen, L.Zhang, "Experimental study on the thermal storage performance and preparation of paraffin mixtures used in the phase change wall", *Solar Energy Materials & Solar Cells*, Vol. 92: 1526–1532, 2008.

48. D. Bentz, R. Turpin, Potential applications of phase change materials in concrete technology, *Cem Concr Compos*, Vol. 29(7):527–32, 2007

49. L. F. Cabeza, C. Castellon, M. Nogues, M. Medrano, R. Leppers, O. Zubillaga, "Use of microencapsulated PCM in concrete walls for energy savings", *Energy and Buildings*, Vol. 39: 113–119, 2007.

50. C. Castellón, M. Medrano, J. Roca, L. F. Cabeza, M. E. Navarro, A. I. Fernández , A. Lázaro, B. Zalba. "Effect of microencapsulated phase change material in sandwich panels", *Renewable Energy*, Vol. 32: 2370–2374, 2010.

51. M. Hunger, A.G. Entrop, I. Mandilaras, H.J.H. Brouwers, M. Founti, "The behavior of self-compacting concrete containing micro-encapsulated Phase Change Materials", *Cement & Concrete Composites*, Vol. 31: 731–743, 2009.

52. C. Chen, L. Wang, Y. Huang, "A novel shape-stabilized PCM: Electrospun ultrafine fibers based on lauric acid/ polyethylene terephthalate composite", *Materials Letters*, Vol. 62: 3515–3517, 2008.

53. C. Chen, L. Wang, Y. Huang, "Ultrafine electrospun fibers based on stearyl stearate/polyethylene terephthalate composite as form stable phase change materials", *Chemical Engineering Journal*, Vol. 150: 269–274, 2009.

54. C. Chen, L.Wang, Y. Huang, Morphology and thermal properties of electrospun fatty acids/polyethylene terephthalate composite fibers as novel form-stable phase change materials, *Sol. Energy Mater. Sol. Cells*, Vol. 92: 1382–1387, 2008.

55. C. Chen, L. Wang, Y. Huang, “Electrospinning of thermo-regulating ultrafine fibers based on polyethylene glycol/cellulose acetate composite”, *Polymer*, Vol. 48: 5202-5207, 2007.

56. C. Chen, L. Wang, Y. Huang, “Crosslinking of the electrospun polyethylene glycol/cellulose acetate composite fibers as shape-stabilized phase change material”, *Materials Letters*, Vol. 63: 569–571, 2009.

57. A. Castell, I. Martorell, M. Medrano, G. Perez, L.F. Cabeza, “Experimental study of using PCM in brick constructive solutions brick constructive solutions for passive cooling”, *Energy and Buildings*, Vol. 42 (4): 534-540, 2010.

58. J. Kosny, D.W. Yarbrough, W. Miller, T. Petrie, P. Childs, A.M. Syed, D. Leuthold, “Thermal performance of PCM-enhanced building envelope systems, in: Thermal Performance of the Exterior Envelopes of Whole Buildings X”, *Proceedings of the ASHRAE/DOE/BTECC Conference*, Clear Water Beach, FL, December 2–7, pp. 1–8, 2007.

59. R. Zeng, X. Wang, B. Chen a, Y. Zhang, J. Niu, Xi. Wang, H. Di, “Heat transfer characteristics of microencapsulated phase change material slurry in laminar flow under constant heat flux”, *Applied Energy*, Vol. 86: 2661–2670, 2009.

60. Y. Zhu, Y. Zhang, G. Li, F. Yang, “Heat transfer processes during an unfixed solid phase change material melting outside a horizontal tube”, *Int. J. Therm. Sci*., Vol. 40: 550–563, 2001.

61. X. Hu, Y. Zhang, “Novel insight and numerical analysis of convective heat transfer enhancement with microencapsulated phase change material slurries: laminar flow in a circular tube with constant heat flux”, *International Journal of Heat and Mass Transfer*, Vol. 45: 3163–3172, 2002.

62. B. Chen, X. Wang, R. Zeng, Y. Zhang, X. Wang, J. Niu, Y. Li, H. Di, “An experimental study of convective heat transfer with microencapsulated phase change material suspension: Laminar flow in a circular tube under constant heat flux”, *Experimental Thermal and Fluid Science*, Vol. 32:1638–1646, 2008.

63. X. Wang, J. Niu, Y. Li, X. Wang, B. Chen, R. Zeng, Q. Song, Y. Zhang, “Flow and heat transfer behaviors of phase change material slurries in a horizontal circular tube”, *International Journal of Heat and Mass Transfer*, Vol. 50: 2480–2491, 2007.

64. M.Ravikumar, PSS. Srinivasan, “Phase change material as a thermal energy storage material for cooling of building”, *Journal of Theoretical and Applied Information Technology*.

65. X. Xu, Y. Zhang, K. Lin, H. Di, R. Yang, “Modeling and simulation on the thermal performance of shape-stabilized phase change material floor used in passive solar buildings”, *Energy and Buildings*, Vol. 37: 1084–1091, 2005.

66. K. Lin, Y. Zhang, X. Xu, H. Di, R. Yang, P. Qin, “Experimental study of under-floor electric heating system with shape-stabilized PCM plates”, *Energy and Buildings*, Vol. 37: 215–220, 2005.

67. G. Zhou, Y. Zhang, Q. Zhang, K. Lin, H. Di, “Performance of a hybrid heating system with thermal storage using shape-stabilized phase-change material plates”, *Applied Energy*, Vol. 84: 1068–1077, 2007.

68. X. Wang, J. Liu, Y. Zhang, Hongfa Di, Yi Jiang, “Experimental research on a kind of novel high temperature phase change storage heater”, *Energy Conversion and Management*, Vol. 47: 2211–2222, 2006.

69. P. Schossig, H. M. Henning, S. Gschwander, T. Haussmann, “Micro-encapsulated phase-change materials integrated into construction materials”, *Solar Energy Materials & Solar Cells*, Vol. 89 297–306, 2005.

70. USG Corperation, URL: http://www.usg.com/, Accessed on October 9, 2011.

71. Microtek Laboratories, Inc., URL: http://www.microteklabs.com/, Accessed on August 27, 2011.

72. BASF, URL: http://www.BASF.com, Accessed on March 23, 2011.

73. C.Y. Zhao, G.H. Zhang, “Review on microencapsulated phase change materials (MEPCMs): Fabrication, characterization and applications”, *Renewable and Sustainable Energy Reviews*, Vol, 15: 3813-3832, 2011.

74. Griffiths, P. De Hasseth, J.A, *Fourier Transform Infrared Spectrometry*, Wiley-Blackwell, 2005.

75. J.F. Su, S.B. Wang, Y. Y. Zhang, Z. Huang, “Physicochemical properties and mechanical characters of methanol-modified melamine-formaldehyde (MMF) shell microPCMs containing paraffin”, *Colloid Polym Sci*, Vol. 289:111–119, 2011.

76. S. H. Lee, “Development of building materials by using micro-encapsulated phase change material”, *Korean J. Chem. Eng*., Vol. 24 (2): 332-335, 2007.

77. G. Tzvetkov, B. Graf, R. Wiegner, J. Raabe, C. Quitmann, R. Fink, “Soft X-ray spectromicroscopy of phase-change microcapsules”, *Micron*, Vol. 39: 275–279, 2008.

78. Mansfield, E.; Kar, A., Quinn, T. P., Hooker, S. A., "Quartz Crystal Microbalances for Microscale Thermogravimetric Analysis”, *Analytical Chemistry* 82 (24), 2010.

79. Dean, John A. *The Analytical Chemistry Handbook*. New York: McGraw Hill, 1995.

80. A. Sharma, S.D. Sharma, D. Buddhi, “Accelerated thermal cycle test of acetamide, stearic acid and paraffin wax for solar thermal latent heat storage applications”, *Energy Conversion and Management*, Vol. 43: 1923–1930, 2002.

81. Xiao-Mei Tong, Ting Zhang, Ming-Zheng Yang, Qiang Zhang, “Preparation and characterization of novel melamine modified poly(urea–formaldehyde) self-repairing microcapsules”, *Colloids and Surfaces A: Physicochem. Eng.*, Vol. 371: 91-97, 2010.

82. "TU Electric Pioneers FGD-Gypsum Production for Use in Wallboard." *Power,* Vol. 4: 33-34, 1988.

83. White, Edwin H. and Mark E. Burger, "Construction Drywall as a Soil Amendment." *BioCycle,* Vol. 7: 70-71, 1993.

84. F.A.L. Dullien, "Porous Media. Fluid Transport and Pore Structure", Academic Press, 1992.

85. J. Temenoff, A. Mikos, “Mechanical Properties of Biomaterials". *Biomaterials - The intersection of Biology and Material Science*. New Jersey: Pearson Prentice Hall Bioengineering, 2008.

86. ASTM Standard: Standard Test Methods for Physical Testing of Gypsum Panel Products, ASTM C473.

87. T. Tritt, Thermal Conductivity: Theory, Properties, and Application, New York: Kluwer Academic/ Plenum Publishers, 2004.

88. ASTM Standard: “Standard Test method for steady state thermal transmission properties by means of the heat flow apparatus,” ASTM C518.

89. Chi-ming Lai, R.H. Chen, Ching-Yao Lin, “Heat transfer and thermal storage behaviour of gypsum boards incorporating micro-encapsulated PCM”, *Energy and Buildings*, Vol. 42: 1259–1266, 2010.

90. Zhi Chen, Guiyin Fang, “Preparation and heat transfer characteristics of microencapsulated phase change material slurry: A review”, *Renew Sustain Energy*, Rev (2011), doi:10.1016/j.rser.2011.07.090.

91. J.P. Holman (2002). *Heat Transfer* (9th ed.). McGraw-Hill, 2002.

92. ASTM Standard: Standard Test Method for Thermal Diffusivity by the Flash Method, ASTM E1461-07

93. J. Goldstein, D. Newbury, D. Joy, C. Lyman, P. Echlin, E. Lifshin, L. Sawyer, J.R. Michael, *Scanning Electron Microscopy and X-ray Microanalysis* (3rd edition), Springer, 2003.